An Appalachian Amazon? Magnetofossil evidence for the development of a tropical river-like system in the mid-Atlantic United States during the Paleocene-Eocene Thermal Maximum

Robert E. Kopp,[1,2] Dirk Schumann,[3] Timothy D. Raub,[4] David S. Powars,[5] Linda V. Godfrey,[6] Nicholas L. Swanson-Hysell,[1] Adam C. Maloof,[1] and Hojatollah Vali[3,7]

On the mid-Atlantic Coastal Plain of the United States, Paleocene sands and silts are replaced during the Paleocene-Eocene Thermal Maximum (PETM) by the kaolinite-rich Marlboro Clay. The clay preserves abundant magnetite produced by magnetotactic bacteria and novel, presumptively eukaryotic, iron-biomineralizing microorganisms. Using ferromagnetic resonance spectroscopy and electron microscopy, we map the magnetofossil distribution in the context of stratigraphy and carbon isotope data and identify three magnetic facies in the clay: one characterized by a mix of detrital particles and magnetofossils, a second with a higher magnetofossil-to-detrital ratio, and a third with only transient magnetofossils. The distribution of these facies suggests that suboxic conditions promoting magnetofossil production and preservation occurred throughout inner-middle neritic sediments of the Salisbury Embayment but extended only transiently to outer neritic sediments and the flanks of the embayment. Such a distribution is consistent with the development of a system resembling a modern tropical river-dominated shelf.

1. Introduction

About 55.6 Ma [*Storey et al.*, 2007], Earth experienced a $\sim 5 - 9°C$ increase in mean global temperature coincident with a -3 to $-5‰$ shift in inorganic carbon isotopes. This warming event, the Paleocene-Eocene Thermal Maximum (PETM), began in less than 10 ky and persisted for about 100–170 ky [*Farley and Eltgroth*, 2003; *Röhl et al.*, 2007]. It is linked to a large injection of isotopically light CO_2 into the global carbon cycle [*Bowen et al.*, 2006], the source of

[1]Department of Geosciences, Princeton University, Princeton, New Jersey, USA

[2]Woodrow Wilson School of Public and International Affairs, Princeton University, Princeton, New Jersey, USA

[3]Department of Earth and Planetary Sciences and Facility for Electron Microscopy Research, McGill University, Montréal, Québec, Canada

[4]Division of Geological and Planetary Sciences, California Institute of Technology, Pasadena, California, USA

[5]U.S. Geological Survey, Reston, Virginia, USA

[6]Institute of Marine and Coastal Sciences, Rutgers University, New Brunswick, New Jersey, USA

[7]Department of Anatomy & Cell Biology, McGill University, Montréal, Québec, Canada

which remains enigmatic; viable hypotheses include thermogenic methane associated with the rifting of Greenland and Scandinavia [*Svensen et al.*, 2004; *Storey et al.*, 2007], sudden exposure and weathering of organic-rich marine sediments [*Higgins and Schrag*, 2006], rapid burning of terrestrial organic carbon [*Kurtz et al.*, 2003] and destabilization of methane clathrates [*Dickens et al.*, 1995]. The warming may have commenced a few ky before the carbon isotope excursion, which would support the hypothesis that methane clathrate destabilization or organic carbon oxidation acted as a feedback that amplified a prior warming [*Sluijs et al.*, 2007].

These and other hypotheses about the cause of the PETM are based primarily on examining carbon isotopic and proxy temperature profiles and identifying potential mechanisms for the observed globally averaged changes. Testing these hypotheses in detail requires understanding the changes in regional environments associated with global climate change. Along the mid-Atlantic Coastal Plain of the United States, for instance, the PETM is accompanied by a radical shift in sedimentation patterns [*Gibson et al.*, 2000]. The sands and silts of the late Paleocene, which biostratigraphic age constraints indicate were deposited at a fairly slow rate [*Van Sickel et al.*, 2004], are replaced by a more rapidly deposited kaolinitic PETM clay. Post-PETM sediments more closely resemble those of the late Paleocene than the PETM clay.

Lanci et al. [2002] and *Kent et al.* [2003] identified an unusual change in rock magnetic properties in the PETM clay in three sediment cores transecting the Coastal Plain in southern New Jersey: Clayton, Ancora, and Bass River (Figure 1a). Late Paleocene and early Eocene sands have low ratios of remanent magnetization (M_r) to saturation magnetization (M_s), consistent with a magnetic mineralogy dominated by multi-domain detrital particles. In the PETM clay, the total amount of magnetic material as reflected by M_s is an order of magnitude larger than in underlying and overlying sediments. The PETM clay also exhibits sustained high M_r/M_s values of ~ 0.3–0.4, indicating

a dominant fraction of fine, single-domain magnetite particles. Indeed, the PETM clay is the thickest single-domain magnetite-dominated sedimentary unit yet reported in the literature.

To explain the magnetic anomaly, *Kent et al.* [2003] suggested that either the single-domain particles could have been produced as impact ejecta condensate, analogous to the magnetic nanophase associated with the Cretaceous-Paleogene boundary [*Wdowiak et al.*, 2001], or they could be magnetofossils, the preserved magnetite crystals produced intracellularly by magnetotactic bacteria. As their transmission electron microscopy (TEM) investigation [*Kent et al.*, 2003] did not reveal particles with the distinctive morphologies and chain arrangements associated with magnetofossils [*Kopp and Kirschvink*, 2008], *Kent et al.* [2003] dismissed the magnetofossil hypothesis in favor of the impact hypothesis [*Cramer and Kent*, 2005]. Other authors [e.g., *Dickens and Francis*, 2004] still preferred a magnetofossil interpretation based on sedimentological arguments.

Re-evaluating the magnetofossil alternative, *Kopp et al.* [2007] examined the PETM clay from Ancora with a combination of electron microscopy and ferromagnetic resonance spectroscopy (FMR), a microwave spectroscopy technique that is sensitive to the shapes, arrangements, and homogeneity characteristic of magnetofossils [*Weiss et al.*, 2004; *Kopp et al.*, 2006a]. These observations, which were supplemented by first-order reversal curve and remanence rock magnetism measurements, showed that the magnetic properties of the PETM clay were produced not by impact ejecta condensate but by an unusual abundance of magnetofossils. *Lippert and Zachos* [2007] came to a similar conclusion using magnetic hysteresis and TEM to investigate the PETM clay at Wilson Lake, a New Jersey drill core site near Clayton.

In modern environments, magnetotactic bacteria live predominantly in the high iron, low oxygen, low sulfide conditions of the oxic/anoxic transition zone, which in different settings can occur either within sediments or within the column [*Kopp and Kirschvink*, 2008]. Similar suboxic conditions foster the preservation of magnetofossils; more strongly reducing conditions promote reductive dissolution of magnetite, while more strongly oxidizing conditions promote its alteration via maghemite to ferric oxides such as goethite and hematite [*Kopp and Kirschvink*, 2008]. *Kopp et al.* [2007] therefore interpreted the high abundance of bacterial magnetofossils in Ancora as reflecting the development of an expanded zone of sedimentary suboxia but could not assess whether the abundance of bacterial magnetofossils was due to syn-depositional changes in growth or to post-depositional changes in preservation.

Subsequent scanning electron microscopy (SEM) and TEM investigations of Ancora sediments resolved the issue of whether the abundance of magnetofossils was solely a preservational effect by identifying "gigantic" multi-micrometer magnetite magnetofossils previously unknown from any modern or ancient environment [*Schumann et al.*, 2008]. These "gigantic" forms include elongated hexaoctahedral, "spindle-shaped," and "spearhead" crystals. Like conventional bacterial magnetofossils, the "gigantic" forms are chemically pure and crystallographically perfect single crystals. Their oxygen isotopic composition is consistent with a low-temperature origin, and the spearheads, in particular, have morphologies and dimensional population statistics that lend themselves to no interpretation other than a biogenic origin. Because of their large size, as well as the observation of a stellate assemblage of spearheads suggestive of an armored protist, these particles are presumed to be eukaryotic rather than bacterial in origin. The discovery of these unique biogenic particles indicates that the abundance of magnetofossils reflected a syn-depositional ecological change, likely linked to a change in the abundance of bio-available iron.

In the modern world, some of the thickest sedimentary suboxic zones occur in tropical river-dominated continental shelves like the Amazon Shelf [*Aller*, 1998] and the Gulf of Papua [*Aller et al.*, 2004a]. *Schumann et al.* [2008] therefore suggested that analogous depositional conditions developed on the Atlantic Coastal Plain during the PETM. This depositional environment would have fostered a thick suboxic zone conducive to the growth and preservation of magnetotactic bacteria and iron-biomineralizing eukaryotes. To test the hypothesis that a tropical, river-dominated shelf could have produced the observed magnetofossil Laagerstätte, we use FMR and electron microscopy (EM) to map the distribution of PETM magnetofossils across the Coastal Plain of the mid-Atlantic United States. We then compare the geographic distribution of magnetofossils to observations of sediments from the modern Amazon Shelf.

2. Geological Setting

The Salisbury Embayment is a deep crystalline basement trough beneath the Coastal Plain of the mid-Atlantic United States [*Richards*, 1948; *Poag and Sevon*, 1989]. The embayment is structurally bounded to the south by the Norfolk Arch [*Gibson*, 1967] and the associated James River structural zone [*Cederstrom*, 1945; *Powars*, 2000] and to the north by the South Jersey High [*Gibson and Bybell*, 1994]. Its western margin is defined by the Fall Line, where the relatively gently dipping Cretaceous and Cenozoic sediments of the Coastal Plain onlap the folded rocks of the Piedmont province.

After a period of rapid post-rift thermal subsidence in the early-middle Jurassic, the Salisbury Embayment has experienced slow subsidence due to cooling and sediment loading [*Kominz et al.*, 2008], possibly combined with epeirogenic subsidence driven by the subduction of the Farallon slab [*Moucha et al.*, 2008; *Müller et al.*, 2008]. The distribution of sediments offshore from the embayment indicates that, since the Jurassic, river systems have flowed into it in positions somewhat similar to those at which the modern Potomac and Susquehanna rivers cross the Fall Line [*Poag and Sevon*, 1989] (Figure 1b).

The paleolatitude of the Salisbury Embayment during the late Paleocene and early Eocene is uncertain. A reconstruction based on sea floor isochrons [*Müller et al.*, 2008] indicates a paleolatitude of ~ 35–$40°$. In contrast, the translation of a high-quality paleopole with a date close to that of the PETM from the Faroe-Rockall Plateau [*Riisager et al.*, 2002] to North America yields a paleolatitude of ~ 25–$28°$ [*Kopp et al.*, 2007]. The discrepancy is currently unexplained [*Ganerød et al.*, 2008]. Hypothesized $\sim 7°$ true polar wander [*Moreau et al.*, 2007], though insufficient to explain the mismatch fully, merits further investigation.

The Salisbury Embayment is divided stratigraphically into a southern domain, spanning the coastal plain of Maryland, Virginia, and Delaware, and a northern domain in New Jersey. In the southern domain, upper Paleocene sediments of the Aquia Formation are predominantly shelly, glauconitic quartz sand and silt. The Aquia Formation is overlain by the Marlboro Clay, a typically massive, 0.1-16 m thick, pink or grey kaolinite-dominated clay layer with occasional thin laminations and thicker beds of silt [*Gibson and Bybell*, 1994]. Although the Aquia/Marlboro contact has been reported as varying between gradational and disconformable [*Gibson and Bybell*, 1994], the contact is always highly burrowed and is interpreted to represent a disconformity across the basin. The Marlboro Clay is in turn disconformably overlain by the Nanjemoy Formation, a glauconitic, sometimes silt-rich or clay-rich quartz sand.

The units in the northern domain are lithologically similar, though typically finer-grained. The upper Paleocene Vincentown Formation, a clay-rich and silt-rich glauconitic fine sand, is overlain by a kaolinite-rich clay unit that has been alternatively described as a member of the Vincentown Formation [e.g., *Miller et al.*, 1998], as a member of the Manasquan Formation [e.g., *Gibson and Bybell*, 1994], or as "the unnamed clay" [e.g., *Miller et al.*, 2006]. This clay, punctuated by rare silt laminations, is overlain by the lower Eocene Manasquan Formation, which in its lower units is characteristically a glauconitic silty clay. Because the Marlboro Clay can be extended from its type area northward on the basis of consistency in lithic characteristics and stratigraphic position, as well as the isotopic and magnetic properties described below, we apply the name "Marlboro Clay" to the initial Eocene clay throughout the Salisbury Embayment.

The Marlboro Clay was deposited across the embayment at inner neritic to outer neritic depths. Based on foraminiferal assemblages, *Gibson and Bybell* [1994] interpreted the Marlboro Clay at Waldorf, MD, and Putneys Mill, VA, as having been deposited under inner neritic depths and inner to middle neritic depths, respectively. *Van Sickel et al.* [2004] estimated that the clay was deposited at about 45–70 m depth at Ancora, NJ, and about 105–135 m depth at Bass River, NJ. Based upon foraminiferal biofacies, Millville, NJ, is estimated to have been deposited at 90–120 m and Sea Girt, NJ, at 80–110 m (A. Harris, unpublished data, 2009).

Microfossil evidence from dinocysts at Bass River, NJ, [*Sluijs et al.*, 2007] and from dinocysts, foraminifera and freshwater algae (*Pseudoschizaea*) at Oak Grove, VA, [*Gibson et al.*, 1980] indicate a significant freshwater flux onto the continental shelf during the PETM. These freshwater indicators are not present before or after the PETM. Fern spores at Oak Grove indicate a moist climate [*Frederiksen*, 1979], while the rapid introduction of seven new sporomorph types in the uppermost Aquia Formation and five more new ones in the lowermost Marlboro Clay [*Frederiksen*, 1979] suggests plant migration driven by climatic changes and/or a shift in sediment source driven by hydrological changes.

3. Methods

3.1. Sampling

3.1.1. Salisbury Embayment

We sampled the late Paleocene through early Eocene sediments of the Salisbury Embayment in ten cores spanning from Busch Gardens in southern Virginia to Sea Girt in central New Jersey (Figure 1a). Except for Busch Gardens, which was drilled by private contractors, cores from Maryland and Virginia were drilled by the U.S. Geological Survey. The four cores from New Jersey were drilled as part of Ocean Drilling Program Leg 174AX. To avoid magnetic contamination, we sampled the cores using non-magnetic tools and scraped outer layers away with plastic implements.

The three most proximal cores are Jackson Landing (J), Randall's Farm (R), and Loretto (L). The present-day altitude of the bottom of the Marlboro Clay at these three sites are respectively 33 m above mean sea level and 16 and 41 m below mean sea level. In contrast to the other localities, at these three sites the Marlboro Clay is predominantly pink in color, although it grades to grey toward the top and sometimes the bottom of the unit. At farther down-basin sites, the Marlboro Clay is almost uniformly grey throughout.

Bass River (BR) is our deepest and most distal locality. The present altitude of the basal Marlboro Clay at BR is 349 m below sea level, compared to 140 to 247 m below

sea level for Ancora (A), South Dover Bridge (SD), Surprise Hill (SH), and Millville (M). The present altitudes of basal Marlboro Clay in Sea Girt (SG) and Busch Gardens (BG) are considerably higher, respectively 114 m and 96 m below sea level. These two sites are distinct in that they sit on the basement highs that bound the Salisbury Embayment; SG is located on the South Jersey High and BG on the Norfolk Arch.

We also collected samples from a section of the Marlboro Clay exposed in outcrop in an artificial ditch in Upper Marlboro, MD, 3 km from R and 9 km from J. The ditch has been subject to surface weathering conditions since at least 2004 and possibly earlier (Mitchell Scott, personal communication, 2008). It exposes 0.9 m of upper Aquia Formation sands and 3.1 m of the Marlboro, predominantly as a massive pink clay that weathers to deep red.

3.1.2. Amazon Shelf

Piston cores of Amazon Shelf sediments were collected in October 1991 as part of the AmasSeds Project [*Nittrouer and DeMaster*, 1996], as described in *Aller et al.* [1996]. The time of sampling was a period of low river flow and low wind stress, and thus near the seasonal maximum of seabed stability. These samples were originally centrifuged for porewater removal and frozen immediately at -20°C in polyethylene bottles. They were kept frozen for sixteen years until analysis. Core RMT-1 comes from a region near the river mouth with sediments composed of thick mud layers interbedded with thin sandy intervals. Cores OST-1 and OST-2 come from a region of the open shelf and consist of more uniform mud.

3.2. Organic carbon

We performed organic carbon isotope analyses on samples from R, L, M, SG and BG. The samples were ground in an agate mortar and pestle and weighed into silver capsules. They then had carbonate removed by adding excess 25% HCl after which they were dried in an oven overnight at 60°C. The carbon isotopic composition of organic matter and organic C concentrations were measured concurrently using a GVI Isoprime CF-IRMS linked to a Eurovector elemental analyzer. (All uses of trade, product, or firm names in this paper are for descriptive purposes only and do not imply endorsement by the U.S. government.) Isotope ratios were corrected against NBS 22 using the accepted value of -30.03‰ [*Coplen et al.*, 2006]. Organic C concentrations were measured using acetanilide and the intensity of masses 44 and 28. Isotope and concentration standards were run following eight sample unknowns.

3.3. Ferromagnetic resonance spectroscopy

Ferromagnetic resonance (FMR) spectra of sediment samples were measured at room temperature using an X-band Bruker EMX spectrometer, following the protocol described in *Kopp et al.* [2006a]. To prepare the samples, approximately 100–400 mg of sediment were lightly crushed in a ceramic mortar.

The shapes of FMR spectra are insensitive to the strength of magnetization so long as samples are neither so weakly magnetized that their spectra are comparable to background noise nor so strongly magnetized such that they saturate the detector; none of the samples we measured fit into either of these two categories. We characterize the spectral shape using two parameters: the asymmetry ratio A and the empirical parameter α [*Kopp et al.*, 2006a]. Spectral asymmetry is sensitive by way of magnetic anisotropy to the shape and arrangements of magnetic particles; $A < 1$ reflects the positive magnetic anisotropy produced by particle elongation or arrangement in chains, while $A > 1$ reflects the negative magnetic anisotropy of a clump of particles. In the

absence of magnetocrystalline anisotropy, isolated particles would have $A = 1$.

The parameter α combines A with the width of a FMR spectrum to produce a proxy for sample homogeneity [*Kopp et al.*, 2006a]. Particles with homogeneous size and shape distributions, such as the characteristic biologically-controlled distributions of magnetofossils, have low α values, while more heterogeneous samples have higher α. Previous observations indicate that $\alpha < 0.25$ characterizes cultures of magnetotactic bacteria and that $\alpha < \sim 0.3$ is characteristic of sediments with magnetic properties dominated by magnetofossils. Sediments with a magnetic mineralogy dominated by detrital particles typically have $\alpha > \sim 0.4$. Mixtures can give rise to intermediate values. All values of α measured to date are between 0.18 and 0.52; see *Kopp et al.* [2006a] and *Kopp et al.* [2006b] for theoretical discussion.

Although the 'gigantic' magnetofossils of *Schumann et al.* [2008] have never been measured in isolation, their elongation and homogeneous size distributions leads us to believe that they would, like other magnetofossils, produce low values of A and α. In any case, the FMR spectra of the Marlboro Clay at Ancora, which contains both 'gigantic' magnetofossils and abundant bacterial magnetofossils, have parameter values expected for magnetofossil-bearing sediments ($A = 0.67$–0.75 and $\alpha = 0.28$–0.30 in the main body of the clay) [*Kopp et al.*, 2007] .

3.4. Electron microscopy

For electron microscopy investigations, the sediment samples were dispersed in distilled water and the magnetic particles extracted using a modified version of the procedure from *Petersen et al.* [1986]. After the sediment samples were gently dispersed in distilled water, they were placed in Petri dishes. The magnetic material was extracted by moving a magnetic finger through the sediment suspension. The magnetic separates were cleaned twice with distilled water and transferred onto 300-mesh Cu TEM grids with carbon support film. SEM observations were then conducted using a Hitachi S-4700 FE-STEM at an accelerating voltage of 5 kV and an emission current of 15 μA. TEM observations were made with a Philips CM200 TEM at 200 kV equipped with an AMT CCD camera.

Magnetic extraction is a necessary step in the microscopic examination of magnetofossils due to their low abundance. For example, in the Marlboro Clay at Ancora, which has M_s of about 10^{-2} Am^2/kg, the concentration of magnetite is about 100 ppm – roughly 10^{-4} times that in a magnetic extract. Our investigations have involved imaging thousands of magnetite particles; it is therefore unsurprising that previous efforts to search for magnetic particles in the clay without an extraction step proved less fruitful [*Kent et al.*, 2003].

The sample preparation procedure, which has been used for over two decades in magnetofossil investigations, is not expected to affect the morphology or chemical composition of individual magnetite particles. At most, dispersion in oxic water might produce a thin, maghemitized oxidation rim, but the timescale for maghemitization at room temperature is slow compared to the duration of the procedure and would not in any case affect morphology or chemical purity.

The formation of linear "strings" of particles [*Kopp et al.*, 2006a] that might be mistaken for biogenic chains is of greater concern and led *Kopp and Kirschvink* [2008] to distinguish between short chain-like structures of ambiguous origins and longer chains composed of particles from a single size and shape distribution. *Kopp and Kirschvink* [2008] also urged that TEM observations of chain-like structures be complemented by techniques, such as FMR, that can provide evidence for their occurrence in unconcentrated samples. The chains reported in *Kopp et al.* [2007] are composed of particles from a single distribution, but their length (up to five particles) places them in an ambiguous position between the two categories. The low A values of the corresponding FMR spectra provides evidence supporting their primary nature.

4. Results

4.1. Organic carbon

All five cores analyzed for bulk organic carbon isotopes exhibit a negative carbon isotope excursion (CIE) within the Marlboro Clay (Figures 2 and 3). The magnitude of the excursion ranges from -1 to $-2‰$ at R to up to $-4.5‰$ at M and SG. The excursion at L (about $-2‰$) and BG (about $-3.5‰$) are intermediate in magnitude. At all sites except R, the excursion takes a form close to that of a step function. The form of the excursion at R is more complicated: a $\sim -0.7‰$ excursion at the base of the Marlboro, followed by a reversion to upper Aquia values, then a gradual decline over the course of the Marlboro Clay to about $-2.1‰$. At all sites, the upper contact of the Marlboro Clay is associated with a sharp but partial return to less negative values.

The concentration of organic carbon (C_{org}) in M and SG increases during the onset of the CIE then returns to pre-CIE concentrations within the remainder of the event. C_{org} in R and L is either unaffected (R) or slightly decreases (L) during the CIE. C_{org} in BG increases stepwise at the start of the CIE. All cores, to a greater (BG) or lesser (SG) extent, exhibit an increase in C_{org} either at or immediately following the end of the CIE (Figure 2). In absolute terms, C_{org} is quite low in late Paleocene sediments and the Marlboro Clay, generally below 0.4 wt%.

4.2. Ferromagnetic resonance
4.2.1. Salisbury Embayment

Above and below the Marlboro Clay, FMR measurements are consistent with a magnetic mineralogy dominated by detrital particles (Figure 2). The mean values of α measured in the late Paleocene and early Eocene units range from 0.40 to 0.43, while mean A values range from 0.90 to 1.05. There is no consistent geographic pattern in the variability of this parameter. In contrast, there are strong geographic patterns in the FMR properties of the Marlboro Clay. On the basis of these properties, we divide the sites into three magnetic facies and two subfacies (Figures 3, 4).

Magnetic facies 1 (R, J, and L): At these sites, the magnetic properties shift at about 10–80 cm above the basal contact of the Marlboro Clay. The shift persists throughout the entire clay layer, although a partial recovery begins 15–150 cm below the upper contact, at similar depths to the shift in color from pink to grey and the first indications of silt-filled burrows. This facies is characterized by a mean α in the Marlboro Clay of 0.34–0.35 and a minimum α of 0.32. Mean A values range from 0.84 to 0.91. These values are consistent with a mixture of magnetofossils and detrital magnetic particles.

Magnetic facies 2 (A, M, SH, and SD): At these sites, the magnetic properties shift in a similar way over the ~ 1 m above the basal contact of the Marlboro Clay, and the shift persists until the first appearance of burrows associated with the overlying unconformity. This facies is characterized by mean α values of 0.30–0.32 and minimum α values of 0.28–0.29. Mean A values range from 0.71 to 0.77. These properties are consistent with a magnetic phase with a stronger dominance by biogenic material relative to detrital magnetic particles than in facies 1. As discussed in *Kopp et al.* [2007],

the zone of high M_r/M_s and high M_s in A [*Kent et al.*, 2003] coincides with the zone of low α values.

Magnetic facies 3 (BR, BG, and SG): At these sites, the shift in FMR properties is not co-extensive with the Marlboro Clay; it is, instead, a transient phenomenon within the clay. As a consequence, mean α values for the Marlboro Clay are high, while the minimum α values are more similar to those of facies 1 and 2. BR (magnetic facies 3a) is characterized by a mean α of 0.36 and a minimum α of 0.29. These values are consistent with the transient occurrence of conditions similar to those in facies 2. BG and SG (magnetic facies 3b) are characterized by mean α values of 0.37–0.38 and a minimum α of 0.31. Mean A values in facies 3 are 0.83–0.85. These values suggest that, during the transient low-α interval, the sediments at these sites contain a greater fraction of detrital particles than facies 2 but less than facies 1. High M_r/M_s and M_s values from the magnetic hysteresis data for BR [*Kent et al.*, 2003] roughly coincide with low α values, though this is challenging to assess both because of variability in the hysteresis and FMR data and because the hysteresis data was not measured through the entire Marlboro Clay.

Although the Upper Marlboro outcrop is located near R and J and is geographically within magnetic facies 1, α values within the Marlboro Clay there are consistently high, with a mean value of 0.40 and a minimum value of 0.36. The magnetofossils of facies 1 thus do not appear to be preserved well in the outcrop. Additional remanence magnetization experiments (see Auxiliary Material) indicate that the magnetization of the Marlboro Clay in outcrop material is an order of magnitude weaker than in core material and that the dominant magnetic phase is not magnetite but a high-coercivity ferric oxide such as goethite.

In many cores in facies 1 and 2, the Marlboro Clay exhibits thin (< 1 m thick) intervals with gradational α values associated with the lower and upper contacts of the unit, as can be seen most clearly in both contacts of R and A and the lower contact of SH. These intervals might reflect either mixing associated with burrowing at the contacts or transitional environmental conditions.

4.2.2. Amazon Shelf

FMR measurements of Amazon Shelf sediment cores are consistent with a magnetic mineralogy consisting of a mixture of detrital grains and conventional bacterial magnetofossils (Figure 6). Sediments from RMT-1 have α values of 0.35–0.39, which are fairly high for samples with significant biogenic magnetite fractions but lower than purely detrital sediments we have previously measured. A values in RMT-1 of 0.80–1.05 also suggest varying biogenic contributions. The two open shelf cores (OST-1 and OST-2) have α values of 0.32–0.34 and A of 0.73–0.85, which indicate a larger and more consistent biogenic fraction.

4.3. Electron microscopy

4.3.1. Salisbury Embayment

Consistent with our previous work on A [*Kopp et al.*, 2007; *Schumann et al.*, 2008], electron microscopy of magnetic extracts from R, SH, SG, and BG confirms that the low values of α observed in the Marlboro Clay reflect a mixture of detrital and biogenic particles (Figure 5; see also Auxiliary Material). In no sample outside the Marlboro Clay did we observe putative eukaryotic magnetofossils or large concentrations of conventional magnetofossils. Similarly, we observed no biogenic magnetite in some of the high-α samples we examined from the Marlboro Clay within magnetic facies 3b (BG-380.30 [depth 115.9 m] and SG-382.45 [depth 116.6 m]).

However, other high-α facies 3b samples we examined did contain putative eukaryotic magnetofossils (BG-400.30 [depth 122.0 m] and SG-366.55 [depth 111.7 m]). These samples are associated with the Aquia/Marlboro contact at BG and the Marlboro/Manasquan contact at SG. The BG sample comes from a gradational contact between the Aquia and the Marlboro Clay and includes a medium-coarse glauconitic sand fraction, while the SG sample comes from an interval with burrows filled by Manasquan sands. In BG-400.30, the high α value is accompanied by apparent dissolution features on the putatively eukaryotic magnetofossils (Figure 5i) and the absence under TEM of conventional magnetofossils . While alteration of the eukaryotic magnetofossils is less severe in SG-366.55, this sample also seems to lack conventional magnetofossils. The presence or absence of conventional magnetofossils thus appears to dominate the FMR properties of the Marlboro Clay. We suggest that the absence of conventional magnetofossils in these two sites is due to the reductive dissolution of magnetite, perhaps facilitated by a preceding period of oxidation associated with burrowing near the contacts.

4.3.2. Amazon Shelf

None of the Amazon Shelf sediment cores contain magnetofossils resembling the "giants" of the Marlboro Clay, but EM reveals a magnetic mineralogy consisting of a mixture of detrital grains and conventional bacterial magnetofossils (Figure 6).

5. Discussion

5.1. Organic carbon

The amplitude of the organic CIE on the mid-Atlantic Coastal Plain is between -2 and $-5‰$. The higher amplitude values are similar to those previously reported from dinocysts at Bass River [*Sluijs et al.*, 2007] and from bulk organic matter in coastal California [*John et al.*, 2008]. The cores exhibiting the lowest amplitude changes are the proximal sites of R and L, where the influence of terrestrial organic carbon is likely strongest. A similarly dampened organic CIE was previously observed in a continental slope section at Tawanui, New Zealand, where the dampening was also attributed to increased terrestrial organic carbon flux [*Crouch et al.*, 2003].

Two terrestrial organic carbon sources may be important contributors to the bulk organic carbon: eroded sedimentary and soil organic matter and land plants. Erosion of sedimentary and soil organic matter formed before the PETM would mask the signal of the CIE. In addition, the C isotopic signature of higher land plants reflects a complex interaction between pCO_2, humidity, and plant species composition. At some localities, these effects combine to dampen the amplitude of changes in $\delta^{13}C$ across the Paleocene-Eocene boundary [*Schouten et al.*, 2007]; this may be the case in the Salisbury Embayment. Regardless of which factor dominates, the gradient in $\delta^{13}C$ is likely related to distance from the mouth of a hypothesized river carrying terrigenous input.

5.2. The distribution of clay, detrital magnetic particles, and magnetofossils

The FMR results can be usefully compared to the distribution of Marlboro Clay thicknesses by considering three fields: the thickness of the Marlboro Clay, the concentration of detrital magnetic particles, and the concentration of magnetofossils. The first we observe directly, while FMR provides a measure of the ratio of the latter two.

In general, the Marlboro Clay thins toward the margins of the Salisbury Embayment, as defined by the Fall Line, the Norfolk Arch, and the South Jersey High, though as

Gibson and Bybell [1994] note, there are also considerable rapid lateral variations in thickness associated with bounding disconformities. The thickest Marlboro Clay interval we measured, at SD, is 15.5 m thick; the thinnest, at L, is 2.7 m thick. The depocenter of the Salisbury Embayment during the PETM is thus in the vicinity of SD (Fig. 1b).

As reflected by the FMR measurements, the ratio of detrital magnetic particles to magnetofossils is higher in magnetic facies 1 than in magnetic facies 2. In magnetic facies 3, this ratio exhibits considerable variability over the course of the PETM, with the minimum value being similar to that of magnetic facies 2 in the case of magnetic facies 3a and intermediate between magnetic facies 1 and 2 in the case of magnetic facies 3b. Throughout the PETM, the mean detrital-to-magnetofossil ratios of magnetic facies 3 exceeds the values in facies 1 and 2.

We interpret the transition from magnetic facies 1 to magnetic facies 2 as being dominated by a change in the concentration of detrital magnetic particles. Due to sorting by grain size and density, the depocenter of detrital magnetic particles would lie closer to the hypothesized river mouth than the depocenter of the clay. Conversely, we interpret the transition from magnetic facies 2 to magnetic facies 3 as being dominated by a change in the concentration of magnetofossils. Magnetic facies 3 is more distal from the hypothesized river mouth than facies 1 or 2, being located either on the outer shelf (facies 3a) or on the flanking highs of the Salisbury Embayment (facies 3b). We suggest that only when conditions were particularly favorable – perhaps during a period of especially strong freshwater flux, or perhaps associated with some other transient environmental change – did the expanded suboxia conducive to the production of biogenic magnetite develop in facies 3. Further supporting the freshwater flux interpretation is evidence from low salinity dinocysts in the Bass River core for an elevated freshwater flux that extends to the outer shelf and peaks in the lower half of the clay interval [*Sluijs et al.*, 2007], much like the magnetofossil anomaly at Bass River (Figure 2).

We note that the broad lateral variability within the three fields discussed here highlights the importance of basinwide analysis in paleoenvironmental reconstruction. Most recent geochemical work and all previous magnetic work on the PETM of the eastern United States has focused on the northern domain of the Salisbury Embayment in New Jersey. This narrow focus has excluded from study all of magnetic facies 1, as well as the depocenter of the Marlboro Clay.

5.3. The meaning of the magnetite

Kopp and Kirschvink [2008] presented a scheme for evaluating putative magnetofossil identifications based upon six categories of criteria: sedimentary context, the presence of a single-domain magnetic phase, particle size and shape, the robustness of evidence for chains, the chemical purity of particles, and the crystallographic perfection of particles. The ranking of the Marlboro Clay bacterial magnetofossils along these axes is discussed in the Auxiliary Material. Previous work [*Lanci et al.*, 2002; *Kent et al.*, 2003; *Kopp et al.*, 2007; *Lippert and Zachos*, 2007] has established the identification of the Marlboro magnetofossils as the second-most robust of all identifications reported in the literature [*Kopp and Kirschvink*, 2008]. Their origin is thus firmly established. Given the absence of modern analogs, the origin of the putatively eukaryotic "gigantic" magnetofossils is harder to establish, but their peculiar shapes, chemical purity, crystallographic perfection, and oxygen isotopic composition compatible with a low-temperature origin all support a biogenic interpretation [*Schumann et al.*, 2008].

The presence of abundant magnetofossils in the Marlboro Clay requires explanations for both their production and their preservation. Magnetotactic bacteria – and presumably other organisms that thrive upon high concentrations of bioavailable Fe – live predominantly within the oxic/anoxic transition zone of sediments and water columns. We have previously interpreted the Marlboro Clay magnetofossils as reflecting expanded sedimentary suboxia [*Kopp et al.*, 2007; *Schumann et al.*, 2008], while *Lippert and Zachos* [2007] preferred to interpret this abundance as an indicator of extensive water column suboxia. Either hypothesis could explain high rates of magnetofossil production.

Although magnetofossil taphonomy is a field with many open questions and only a handful of empirical studies in modern environments [e.g., *Snowball*, 1994; *Kodama*, 2006; *Housen and Moskowitz*, 2006; *Maloof et al.*, 2007], magnetofossil preservation is readily explained in the case of sedimentary suboxia. If electron-donor limitation occurs within the suboxic, iron-reducing zone of sediments, magnetite will not be efficiently reduced to Fe(II) and thus will be preserved.

Preservation is harder to explain in the case of expanded water-column suboxia. Organic carbon fluxes sufficient to drive the development of suboxic conditions within the water column will tend to produce fully anoxic conditions within the sediments. Such conditions are not conducive to the preservation of fine-grained magnetite, the dissolution of which has been observed in anoxic freshwater [*Snowball*, 1994; *Kodama*, 2006] and marine [*Maloof et al.*, 2007] sediments with a timescale of a few centuries. *Dickens* [2008] suggested that non-steady-state redox conditions might have allowed high-Fe, high-C, non-sulfidic sediments deposited during the PETM to overlay late Paleocene sediments with low-Fe, low-C, oxic-to-suboxic porewaters and thus isolate the magnetofossils from sulfidic conditions. Such isolation is, however, insufficient to protect magnetofossils from dissolution; in the absence of sulfide but the presence of sufficient electron donors (i.e., organic carbon), iron-reducing bacteria will catalyze the reductive dissolution of fine-grained magnetite, as has been observed both in laboratory cultures [*Kostka and Nealson*, 1995; *Dong et al.*, 2000] and in sedimentary profiles of magnetofossil abundance [*Tarduno*, 1994; *Housen and Moskowitz*, 2006]. The balance of evidence thus currently favors interpreting abundant ancient magnetofossils as indicators of expanded sedimentary suboxia.

5.4. The tropical river-dominated shelf analog

The hypothesis that the bloom of iron biomineralizing organisms on the Atlantic Coastal Plain was caused by the development of conditions similar to a tropical river-dominated shelf is based upon the observation of extremely thick sedimentary suboxic zones in these modern analog environments. For example, in one piston-core from the Amazon Shelf (RMT-2; Figure 6), located at ~ 20 m water depth and a bit over 100 km offshore from the river mouth, an oxygen-free zone of high and increasing Fe^{2+} concentration extends through the top ~ 4 m of sediment [*Aller et al.*, 1996]. In the upper 2 m, SO_4^{2-} concentrations are nearly constant, indicating that Fe^{3+} is the main electron acceptor; and even at lower depths, the degree of pyritization is extremely low, never exceeding 0.05 [*Aller and Blair*, 1996]. The thick suboxic zone is due to a combination of factors including moderately high concentrations of reactive Fe [*Aller et al.*, 2004b] and a high-energy environment produced by tides, frontal-zone currents, and surface waves [*Nittrouer and DeMaster*, 1996]. These latter processes promote the regular physical reworking of the top ~ 1 m of sediments, which allows the re-oxidation of reduced Fe, thereby increasing the availability of Fe as an electron acceptor.

Like the Marlboro Clay, Amazon Shelf sediments are dominated by fine particles; 85–95% of the sediment discharged by the Amazon River is clay-sized or silt-sized [*Kuehl et al.*, 1986]. The dominant clay minerals on the Amazon Shelf are kaolinite and montmorillonite [*Gibbs*, 1967]. Modern deposition of clay and silt occurs laterally across the inner shelf, while sand deposition, driven by outflow turbulence, is confined to a corridor of interbedded sand and mud extending from the river mouth [*Nittrouer et al.*, 1983].

During the PETM, the paleo-Potomac River or the paleo-Susquehanna River [*Poag and Sevon*, 1989] (Figure 1b) may have played a role analogous to that of the Amazon River and would have promoted a similarly thick suboxic zone. In general, the distribution of sediments offshore from the Salisbury Embayment indicates that the paleo-Potomac was active during the late Cretaceous but relatively quiescent from the Paleocene and early Eocene, while the paleo-Susquehanna was particularly active in the Paleocene [*Poag and Sevon*, 1989]. However, these results represent only averages of deposition over geological epochs. Moreover, a sand bank complex in the Aquia Formation appears to have been deposited by the paleo-Potomac in the late Paleocene, which indicates some degree of continued activity [*Hansen*, 1974]. The temperature and precipitation changes associated with the PETM would have altered the hydrological cycle and could have re-intensified the flow of the paleo-Potomac. Consistent with the paleo-Potomac model is the stronger dilution of the biogenic signal by detrital input in magnetic facies 1. However, our cores do not include similarly shallow sediments in the northern Salisbury Embayment, where the influence of the paleo-Susquehanna might be recorded.

High delivery of Fe to the continental shelf during the PETM may have been promoted by increased temperatures and more acidic rainwater. Warm, humid conditions like those of modern tropical environments promote the leaching of Fe during soil formation processes, as do rain and groundwater acidity. These conditions also promote the formation of clay minerals, particularly cation-depleted ones like kaolinite. A high energy shelf environment, capable of driving the physical reworking that helps maintain suboxia, may have developed as a result of changes in ocean or atmospheric circulation. Though unchanged during the PETM, the structure of the embayment might also have contributed to maintaining a high energy environment by resonant amplification of tidal energy.

One possible objection to the Amazon analogy involves deposition rate. Assuming the Marlboro Clay at each locality preserves a complete record of the ~ 70–~ 90 ky duration of the main CIE [*Farley and Eltgroth*, 2003; *Röhl et al.*, 2007] and decompacting the sediments using the porosity v. depth curves of *Van Sickel et al.* [2004], then the deposition rate of the clay ranges from $\sim$3.9–4.1 cm/ky at L to $\sim$25.6–29.6 cm/ky at SD. These rates reflect a significant increase above the rather slow background Paleocene–Eocene deposition rate. At A, for instance, the deposition rate of $\sim$9.1–10.3 cm/ky is an order of magnitude larger than the background rate of $\sim$0.5–1.0 cm/ky, estimated from biostratigraphy and magnetostratigraphy [*Van Sickel et al.*, 2004]. However, even the elevated PETM rates are not exceptionally high. By contrast, deposition rates on the modern Amazon shelf can exceed $\sim 10^4$ cm/ky [*Kuehl et al.*, 1986].

Such rates, however, reflect only short-term processes. Long-term accumulation rates are controlled by subsidence rates, which on the Amazon Shelf have averaged about 15–22 cm/ky since the Miocene [*Kumar et al.*, 1977]. Over shorter periods of time, different localities on the shelf alternate between multi-century intervals of net accretion and multi-century intervals of net erosion [*Nittrouer et al.*, 1996]. Similarly, there is no reason to expect the Marlboro Clay at any locality to preserve a complete record of the PETM. Though at some localities the basal contact of the Marlboro Clay appears gradational and might reflect continuous deposition (but also might instead reflect extensive bioturbation), the top of the Marlboro Clay is always characterized by an erosional unconformity [*Gibson and Bybell*, 1994]. The apparent gradual termination of the carbon isotope excursion at some localities could be a product of mixing driven by bioturbation. Our depositional model further suggests that the Marlboro Clay should contain numerous disconformities, and the physical mixing predicted by our model is consistent with the unit's generally massive appearance.

5.5. Comparison to the modern Amazon shelf

As in the Marlboro Clay, magnetic particles on the Amazon shelf are a mixture of detrital and biogenic particles. Near the river mouth, the detrital-to-magnetofossil ratio is higher than at the open shelf sites, which have α values similar to those of Marlboro magnetic facies 1. The two open shelf cores are, however, located farther laterally from the river mouth than the facies 1 cores are from the paleo-Potomac. These results suggest a lower detrital-to-magnetofossil ratio in the Marlboro Clay than on the Amazon Shelf, perhaps reflecting a lower riverine sediment flux and potentially a higher flux and/or concentration of dissolved Fe (Figure 6).

The scale of the Salisbury Embayment compared to the Amazon Shelf is consistent with a lower riverine sediment flux from the paleo-Potomac than from the modern Amazon. The region of clay deposition on the Amazon Shelf, which extends roughly from the mouth of the Para River in the south to Cabo Orange in the north, is about 650 km in width [*Nittrouer et al.*, 1983]. By comparison, the Salisbury Embayment is about 400 km in width. Volume scaling suggests that environmental conditions similar to those of the Amazon Shelf might therefore have been maintained in the Salisbury Embayment with about one-quarter the riverine input. Also compatible with a smaller sediment flux, Millville, which is about 50 km from the Fall Line, has an estimated paleodepth of 90–120 m. On the Amazon Shelf north of the river mouth, a comparable distance offshore yields a water depth between 10 and 60 m [*Aller et al.*, 1996].

A sediment flux into the Salisbury Embayment equal to about one-quarter of that of the Amazon could have been produced by a few flood events each year similar in scale to those produced by hurricanes today. (See the Auxiliary Material for an order-of-magnitude calculation.) Hurricane exposure of this frequency is consistent with the hypothesis that increased tropical cyclone activity was responsible for a reduced pole-to-equator gradient during the PETM [*Korty et al.*, 2008; *Sluijs et al.*, 2007]. Alternatively, these flood events might have been of lesser magnitude but more protracted duration, consistent with suggestions of monsoonal precipitation patterns [*Zachos et al.*, 2006].

The lower detrital-to-magnetofossil ratio in the sediments in the Salisbury Embayment as compared to the Amazon Shelf could reflect a higher ratio of reactive Fe flux to total sediment flux. This high ratio could have resulted from more intense chemical weathering, perhaps a product of high CO_2 concentrations and consequently more acidic rainwater. Alternatively, the erosion of Cretaceous-age Coastal Plain deposits that had undergone millions of years of chemical weathering, such as the kaolinite-rich deltaic clays of the Raritan Formation [*Groot and Glass*, 1960], could have enhanced reactive iron fluxes. Ocean acidification could also have increased iron concentrations [*Breitbarth et al.*, 2009].

Although we did not find "gigantic" magnetofossils in the three Amazon Shelf piston-cores we examined, the "giants" could still exist the modern world. Aside from our limited analysis, we are unaware of any other electron microscopy study of the magnetic mineralogy of the suboxic zones of tropical river shelf sediments. The problem thus suffers from undersampling. However, it is also possible that these magnetofossils were produced by extinct organisms, in which case the best hope for understanding them lies in more thorough development of the magnetofossil record.

5.6. Uniqueness of the Marlboro Clay within the Salisbury Embayment

During the Early Eocene Climatic Optimum (EECO) at 51–53 Ma, global temperatures were comparable to those of the PETM [*Zachos et al.*, 2008]. As EECO came only about 4 My after the PETM, the paleogeographic location of the Salisbury Embayment would have been quite similar. Yet, despite the extended duration of the climatic optimum, no sedimentologically and magnetically anomalous clay layer akin to the Marlboro Clay is associated with it [*Gibson and Bybell*, 1994; *Lanci et al.*, 2002]. This absence suggests that the rate of warming, not simply the degree of warming, was instrumental in the formation of the Marlboro Clay. Perhaps the more protracted EECO warming affected oceanic and atmospheric circulation in a different fashion; or perhaps a similar layer did form briefly during EECO but was then eroded away, and the shorter duration of the PETM was necessary for the preservations of the clay. Alternatively, if the availability of Cretaceous clay for weathering played an important role in the formation of the Marlboro Clay, then the removal of the Cretaceous clay during the PETM may have prevented the later re-establishment of a similar sedimentary system.

In addition to the long-lived EECO, short-lived hyperthermal events similar in duration to but smaller in magnitude than the PETM also occurred during the early Eocene [*Nicolo et al.*, 2007]. Although no magnetofossil anomaly associated with these events has been found in the Salisbury Embayment, much of the early Eocene Manasquan Formation is clay dominated, and it is possible that the magnetic susceptibility survey of *Lanci et al.* [2002] could have missed a magnetic anomaly of smaller magnitude than that of the Marlboro Clay.

5.7. Global implications

Because of their high deposition rates, river-dominated continental shelves play an important role in the modern global carbon cycle and collectively account for about 45% of all marine organic carbon burial [*Hedges and Keil*, 1995; *Aller and Blair*, 2006]. Yet because of the same processes that give rise to thick suboxic zones, they are also highly effective at remineralizing organic carbon; they constitute a "global incineration zone" with low ratios of organic carbon concentration to sediment surface area [*Aller and Blair*, 2006]. Processes that alter biogeochemical cycling in these areas can therefore have strong positive or negative effects on global carbon burial. The biogeochemical shift reflected in the Marlboro Clay might therefore have been part of a global carbon cycle feedback [*John et al.*, 2008]. The sign of such a feedback is ambiguous: high deposition rates could have driven a negative feedback, while the high efficiency of organic carbon oxidation could have driven a positive feedback. The potential magnitude of this feedback depends in part upon whether the changes observed on the Atlantic Coastal Plain during the PETM are solely regional or are one example of many such environments that developed during the PETM.

Some of the factors we suggest contribute to the development of the Marlboro biogeomagnetic anomaly are global in nature, such as increased temperatures and more acidic rain. The hydrological changes resulting in increased sediment flux to continental shelves are similarly observed in other regions during the PETM [e.g., *Schmitz and Pujalte*, 2003; *Giusberti et al.*, 2007], as is elevated kaolinite deposition [e.g., *Robert and Kennett*, 1994; *Bolle et al.*, 2000]. In contrast, the effects of changes in sediment source and in atmospheric and oceanic circulation will exhibit regional variation. To determine whether the changes in the iron cycle observed in the Marlboro reflect an event unique to the Atlantic Coastal Plain or a global trend requires comparable investigations of neritic PETM sediments in other parts of the world, such as the Spanish Pyrenees [*Schmitz and Pujalte*, 2007] and Tanzania [*Nicholas et al.*, 2006].

To direct these investigations, it is useful to know the conditions under which a biogeomagnetic anomaly like that of the Marlboro Clay can be preserved. In the Upper Marlboro outcrop, which is located within ten kilometers of both R and J, the magnetofossil signal has been lost to oxidation. This oxidation could have resulted either from surface weathering in the years since the excavation of the ditch or from millennia sitting within meters of the surface and associated soil formation processes. In either case, this result suggests that a feature like the Marlboro anomaly is much more easily identified using samples from drill cores or locations that have never been exposed to oxidative surface weathering or soil formation. Such samples should therefore be the focus of future investigations into iron cycle changes during the PETM.

6. Conclusions

Like the Marlboro Clay, the conditions of expanded sedimentary suboxia that promoted the growth of magnetotactic bacteria and more unusual, likely eukaryotic, iron-biomineralizing organisms, as well as the preservation of the magnetite they produced, spanned the Salisbury Embayment during the PETM. However, in some locations the magnetic anomaly persists for only a portion of the thickness of the clay. The partial independence of the anomaly from sedimentary lithology provides further evidence that the biogeomagnetic anomaly was in large part a syn-depositional growth phenomenon, rather than purely a preservational phenomenon linked to the lithologic change.

Coincident with the global carbon isotope excursion, regional changes in hydrology and weathering conditions initiated deposition of the Marlboro Clay. The onset of suboxic conditions promoting iron biomineralization may have slightly lagged the depositional change, but these conditions persisted for most of the PETM in the inner and middle neritic sediments of the Salisbury Embayment. They extended only transiently to the outer neritic region and onto the flanks of the Norfolk Arch and the South Jersey High.

Combined with the distribution of detrital magnetic minerals and independent evidence for a strong freshwater flux onto the shelf, the distribution of suboxia supports the hypothesis that conditions akin to those of a modern tropical river-dominated shelf developed on the Atlantic Coastal Plain. The high sediment flux associated with these conditions might be linked to intensified precipitation, perhaps tied either to monsoonal precipitation patterns or more frequent tropical cyclones. A high flux of reactive iron could have resulted from enhanced chemical weathering under hot, high-CO_2 conditions. The mid-Atlantic United States thus provides one example of the severe regional environmental changes associated with global climate change during the PETM. Both modeling studies and further geological work across the region can improve understanding of the forces driving these changes, as well as the successes and limitations of the tropical river-dominated shelf analog.

References

Aller, R. C. (1998), Mobile deltaic and continental shelf muds as suboxic, fluidized bed reactors, *Mar. Chem.*, *61*, 143–155.

Aller, R. C., and N. E. Blair (1996), Sulfur diagenesis and burial on the Amazon shelf: Major control by physical sedimentation processes, *Geo-Mar. Lett.*, *16*, 3–10.

Aller, R. C., and N. E. Blair (2006), Carbon remineralization in the Amazon–Guianas tropical mobile mudbelt: A sedimentary incinerator, *Cont. Shelf Res.*, *26*, 2241–2259.

Aller, R. C., N. E. Blair, Q. Xia, and P. D. Rude (1996), Remineralization rates, recycling, and storage of carbon in Amazon shelf sediments, *Cont. Shelf Res.*, *16*, 753–786.

Aller, R. C., A. Hannides, C. Heilbrun, and C. Panzeca (2004a), Coupling of early diagenetic processes and sedimentary dynamics in tropical shelf environments: the Gulf of Papua deltaic complex, *Cont. Shelf Res.*, *24*, 2455–2486.

Aller, R. C., C. Heilbrun, C. Panzeca, Z. Zhu, and F. Baltzer (2004b), Coupling between sedimentary dynamics, early diagenetic processes, and biogeochemical cycling in the Amazon–Guianas mobile mud belt: coastal French Guiana, *Mar. Geology*, *208*, 331–360.

Bolle, M. P., A. Pardo, T. Adatte, K. von Salis, and S. Burns (2000), Climatic evolution on the southeastern magin of the Tethys (Negev, Israel) from the Palaeocene to the early Eocene: focus on the late Palaeocene thermal maximum, *J. Geol. Soc. London*, *157*, 929–941.

Bowen, G. J., et al. (2006), Eocene hyperthermal event offers insight into greenhouse warming, *Eos Trans. AGU*, *87*, 165, 169.

Breitbarth, E., R. J. Bellerby, C. C. Neill, M. V. Ardelan, M. Meyerhöfer, E. Zöllner, P. L. Croot, and U. Riebesell (2009), Ocean acidification affects iron speciation in seawater, *Biogeosciences Diss.*, *6*, 6781–6802.

Cederstrom, D. J. (1945), Structural geology of southeastern Virginia, *AAPG Bull.*, *29*, 71–95.

Coplen, T. B., W. A. Brand, M. Gehre, M. Groning, H. A. J. Meijer, B. Toman, and R. M. Verkouteren (2006), New guidelines for $\delta^{13}C$ measurements, *Anal. Chem.*, *78*, 2439–2441.

Cramer, B. S., and D. V. Kent (2005), Bolide summer: The Paleocene/Eocene thermal maximum as a response to an extraterrestrial trigger, *Palaeogeog. Palaeoclim. Palaeoecol.*, *224*, 144–166.

Crouch, E. M., G. R. Dickens, H. Brinkhuis, M. Aubry, C. J. Hollis, K. M. Rogers, and H. Visscher (2003), The Apectodinium acme and terrestrial discharge during the Paleocene-Eocene thermal maximum: new palynological, geochemical and calcareous nannoplankton observations at Tawanui, New Zealand, *Palaeogeog. Palaeoclim. Palaeoecol.*, *194*, 387–403.

Dickens, G. R. (2008), Palaeoclimate: The riddle of the clays, *Nat. Geosci.*, *1*, 86–88.

Dickens, G. R., and J. M. Francis (2004), Comment on "A case for a comet impact trigger for the Paleocene/Eocene thermal maximum and carbon isotope excursio" by DV Kent et al.[Earth Planet. Sci. Lett. 211 (2003) 13–26], *Earth Planet. Sci. Lett.*, *217*, 197–200.

Dickens, G. R., J. R. O'Neil, D. K. Rea, and R. M. Owen (1995), Dissociation of oceanic methane hydrate as a cause of the carbon isotope excursion at the end of the Paleocene, *Paleoceanography*, *10*, 965–971.

Dong, H., J. K. Fredrickson, D. W. Kennedy, J. M. Zachara, R. K. Kukkadapu, and T. C. Onstott (2000), Mineral transformation associated with the microbial reduction of magnetite, *Chem. Geol*, *169*, 299–318.

Farley, K. A., and S. F. Eltgroth (2003), An alternative age model for the Paleocene-Eocene thermal maximum using extraterrestrial He-3, *Earth Planet. Sci. Lett.*, *208*, 135–148.

Frederiksen, N. O. (1979), Paleogene sporomorph biostratigraphy, northeastern Virginia, *Palynology*, *3*, 129–167.

Ganerød, M., M. A. Smethurst, S. Rousse, T. H. Torsvik, and T. Prestvik (2008), Reassembling the Paleogene–Eocene North Atlantic igneous province: New paleomagnetic constraints from the Isle of Mull, Scotland, *Earth Planet. Sci. Lett.*, *272*, 464–475.

Gibbs, R. J. (1967), The geochemistry of the Amazon river system; part I, The factors that control the salinity and the composition and concentration of the suspended solids, *Bull. Geol. Soc. Am.*, *78*, 1203–1232.

Gibson, T. G. (1967), Stratigraphy and paleoenvironment of the phosphatic Miocene strata of North Carolina, *Bull. Geol. Soc. Am.*, *78*, 631–650.

Gibson, T. G., and L. M. Bybell (1994), Sedimentary patterns across the Paleocene–Eocene boundary in the Atlantic and Gulf Coastal Plains of the United States, *Bull. de la Société belge de Géologie*, *103*, 237–256.

Gibson, T. G., G. W. Andrews, L. M. Bybell, N. O. Frederiksen, T. Hansen, J. E. Hazel, D. M. Mclean, R. J. Witmer, and D. S. Van Nieuwenhu (1980), Biostratigraphy of the Tertiary strata of the core, in *Geology of the Oak Grove core*, pp. 14–30, Virginia Division of Mineral Resources.

Gibson, T. G., L. M. Bybell, and D. B. Mason (2000), Stratigraphic and climatic implications of clay mineral changes around the Paleocene/Eocene boundary of the northeastern US margin, *Sed. Geol.*, *134*, 65–92.

Giusberti, L., D. Rio, C. Agnini, J. Backman, E. Fornaciari, F. Tateo, and M. Oddone (2007), Mode and tempo of the Paleocene-Eocene thermal maximum in an expanded section from the Venetian pre-Alps, *Bull. Geol. Soc. America*, *119*, 391–412.

Groot, J. J., and H. D. Glass (1960), Some aspects of the mineralogy of the northern Atlantic Coastal Plain, in *Clays and Clay Minerals: Proc. Seventh National Conference on Clays and Clay Minerals*, edited by A. Swineford, pp. 271–284, Pergamon Press, New York.

Hansen, H. J. (1974), Sedimentary facies of the Aquia formation in the subsurface of the Maryland Coastal Plain, *Report of Investigations 21*, Maryland Geological Survey.

Hedges, J. I., and R. G. Keil (1995), Sedimentary organic matter preservation: An assessment and speculative synthesis, *Mar. Chem.*, *49*, 81–115.

Higgins, J. A., and D. P. Schrag (2006), Beyond methane: Towards a theory for the Paleocene-Eocene Thermal Maximum, *Earth Planet. Sci. Lett.*, *245*, 523–537.

Housen, B. A., and B. M. Moskowitz (2006), Depth distribution of magnetofossils in near-surface sediments from the blake/bahama outer ridge, western north atlantic ocean, determined by low-temperature magnetism, *J. Geophys. Res.*, *111*, G01005, doi:10.1029/2005JD005776.

John, C. M., S. M. Bohaty, J. C. Zachos, A. Sluijs, S. Gibbs, H. Brinkhuis, and T. J. Bralower (2008), North American continental margin records of the Paleocene-Eocene thermal

maximum: Implications for global carbon and hydrological cycling, *Paleoceanography*, *23*, PA2217, doi: 10.1029/2007PA001465.

Kent, D. V., B. S. Cramer, L. Lanci, D. Wang, J. D. Wright, and R. Van der Voo (2003), A case for a comet impact trigger for the Paleocene/Eocene thermal maximum and carbon isotope excursion, *Earth Planet. Sci. Lett.*, *211*, 13–26.

Kodama, K. P. (2006), The role of magnetosomes in the sediments of Lake Ely, PA: Their production and destruction, *Geol. Soc. America Abstracts with Programs*, *38*, 200.

Kominz, M. A., J. V. Browning, K. G. Miller, P. J. Sugarman, S. Mizintseva, and C. R. Scotese (2008), Late Cretaceous to Miocene sea-level estimates from the New Jersey and Delaware coastal plain coreholes: an error analysis, *Basin Res.*, *20*, 211–226.

Kopp, R. E., and J. L. Kirschvink (2008), The identification and biogeochemical interpretation of fossil magnetotactic bacteria, *Earth-Sci. Rev.*, *86*, 42–61.

Kopp, R. E., B. P. Weiss, A. C. Maloof, H. Vali, C. Z. Nash, and J. L. Kirschvink (2006a), Chains, clumps, and strings: Magnetofossil taphonomy with ferromagnetic resonance spectroscopy, *Earth Planet. Sci. Lett.*, *247*, 10–25.

Kopp, R. E., C. Z. Nash, A. Kobayashi, B. P. Weiss, D. A. Bazylinski, and J. L. Kirschvink (2006b), Ferromagnetic resonance spectroscopy for assessment of magnetic anisotropy and magnetostatic interactions: A case study of mutant magnetotactic bacteria, *J. Geophys. Res.*, *111*, B12S25, doi:10.1029/2006JB004529.

Kopp, R. E., T. D. Raub, D. Schumann, H. Vali, A. V. Smirnov, and J. L. Kirschvink (2007), Magnetofossil spike during the Paleocene-Eocene thermal maximum: Ferromagnetic resonance, rock magnetic, and electron microscopy evidence from Ancora, New Jersey, United States, *Paleoceanography*, *22*, PA4103, doi:10.1029/2007PA001473.

Korty, R. L., K. A. Emanuel, and J. R. Scott (2008), Tropical cyclone–induced upper-ocean mixing and climate: Application to equable climates, *J. Climate*, *21*, 638–654.

Kostka, J. E., and K. H. Nealson (1995), Dissolution and reduction of magnetite by bacteria, *Environmental Science & Technology*, *29*, 2535–2540.

Kuehl, S. A., D. J. DeMaster, and C. A. Nittrouer (1986), Nature of sediment accumulation on the Amazon continental shelf, *Cont. Shelf Res.*, *6*, 209–225.

Kumar, N., J. E. Damuth, and M. A. Gorini (1977), Discussion – Relict magnesian calcite oolite and subsidence of the Amazon shelf, *Sedimentology*, *24*, 143–148.

Kurtz, A. C., L. R. Kump, M. A. Arthur, J. C. Zachos, and A. Paytan (2003), Early Cenozoic decoupling of global carbon and sulfur cycles, *Paleoceanography*, *18*, 1090, doi: 10.1029/2003PA000908.

Lanci, L., D. V. Kent, and K. G. Miller (2002), Detection of Late Cretaceous and Cenozoic sequence boundaries on the Atlantic coastal plain using core log integration of magnetic susceptibility and natural gamma ray measurements at Ancora, New Jersey, *J. Geophys. Res.*, *107*, 2216, doi:10.1029/2000JB000026.

Lippert, P. C., and J. C. Zachos (2007), A biogenic origin for anomalous fine-grained magnetic material at the Paleocene-Eocene boundary at Wilson Lake, New Jersey, *Paleoceanography*, *22*, PA4104, doi: 10.1029/2007PA001471.

Maloof, A. C., R. E. Kopp, J. P. Grotzinger, D. A. Fike, T. Bosak, H. Vali, P. M. Poussart, B. P. Weiss, and J. L. Kirschvink (2007), Sedimentary iron cycling and the origin and preservation of magnetization in platform carbonate muds, Andros Island, Bahamas, *Earth Planet. Sci. Lett.*, *259*, 581–598.

Miller, K. G., et al. (1998), Bass River Site, *Proc. Ocean Drilling Program, Initial Reports*, *174AX*, 5–43.

Miller, K. G., et al. (2006), Sea Girt Site, *Proc. Ocean Drilling Program, Initial Reports*, *174AX (Suppl.)*, 1–104, doi: 10.2973/odp.proc.ir.174AXS.107.2006.

Mixon, R. B., and D. S. Powars (1984), Folds and faults in the inner Coastal Plain of Virginia and Maryland: Their effect on the distribution and thickness of Tertiary rock units and local geomorphic history, in *Cretaceous and Tertiary stratigraphy, plaeontology, and structure, southwestern Maryland and northeastern Virginia; Field trip volume and guidebook*, edited by N. Fredericksen and K. Krafft, pp. 112–122, American Association of Stratigraphic Palynologists.

Moreau, M., J. Besse, F. Fluteau, and M. Greff-Lefftz (2007), A new global Paleocene–Eocene apparent polar wandering path loop by "stacking" magnetostratigraphies: Correlations with high latitude climatic data, *Earth Planet. Sci. Lett.*, *260*, 152–165.

Moucha, R., A. M. Forte, J. X. Mitrovica, D. B. Rowley, S. Quéré, N. A. Simmons, and S. P. Grand (2008), Dynamic topography and long-term sea-level variations: There is no such thing as a stable continental platform, *Earth Planet. Sci. Lett.*, *271*, 101–108.

Müller, R. D., M. Sdrolias, C. Gaina, B. Steinberger, and C. Heine (2008), Long-term sea-level fluctuations driven by ocean basin dynamics, *Science*, *319*, 1357–1362.

Nicholas, C. J., et al. (2006), Stratigraphy and sedimentology of the Upper Cretaceous to Paleogene Kilwa Group, southern coastal Tanzania, *J. Afr. Earth Sci.*, *45*, 431–466.

Nicolo, M. J., G. R. Dickens, C. J. Hollis, and J. C. Zachos (2007), Multiple early Eocene hyperthermals: Their sedimentary expression on the New Zealand continental margin and in the deep sea, *Geology*, *35*, 699–702.

Nittrouer, C. A., and D. J. DeMaster (1996), The Amazon shelf setting: tropical, energetic, and influenced by a large river, *Cont. Shelf Res.*, *16*, 553–573.

Nittrouer, C. A., M. T. Sharara, and D. J. DeMaster (1983), Variations of sediment texture on the Amazon continental shelf, *J. Sed. Res.*, *53*, 179–191.

Nittrouer, C. A., S. A. Kuehl, A. G. Figueiredo, M. A. Allison, C. K. Sommerfield, J. M. Rine, L. E. C. Faria, and O. M. Silveira (1996), The geological record preserved by Amazon shelf sedimentation, *Cont. Shelf Res.*, *16*, 817–841.

Petersen, N., T. Vondobeneck, and H. Vali (1986), Fossil bacterial magnetite in deep-sea sediments from the South Atlantic Ocean, *Nature*, *320*, 611–615.

Poag, C. W., and W. D. Sevon (1989), A record of Applachian denudation in postrift Mesozoic and Cenozoic sedimentary deposits of the U.S. middle Atlantic continental margin, *Geomorphology*, *2*, 119–157.

Powars, D. S. (2000), The effects of the Chesapeake Bay impact crater on the geological framework and the correlation of hydrological units of southeastern Virginia, south of the James River, *Professional Paper 1622*, United States Geological Survey.

Powars, D. S., and T. S. Bruce (1999), The effects of the Chesapeake Bay impact crater on the geological framework and correlation of hydrological units of the Lower York–James Peninsula, Virginia, *Professional Paper 1612*, United States Geological Survey.

Richards, H. G. (1948), Studies of the geology and paleontology of the Atlantic Coastal Plain, *Proc. Academy of Natural Sciences of Philadelphia*, *100*, 39–76.

Riisager, P., J. Riisager, N. Abrahamsen, and R. Waagstein (2002), New paleomagnetic pole and magnetostratigraphy of Faroe Islands flood volcanics, North Atlantic igneous province, *Earth Planet. Sci. Lett.*, *201*, 261–276.

Robert, C., and J. P. Kennett (1994), Antarctic subtropical humid episode at the Paleocene-Eocene boundary–clay mineral evidence, *Geology*, *22*, 211–214.

Röhl, U., T. Westerhold, T. J. Bralower, and J. C. Zachos (2007), On the duration of the Paleocene-Eocene thermal maximum (PETM), *Geochem. Geophys. Geosys.*, *8*, Q12002, doi: 10.1029/2007GC001784.

Schmitz, B., and V. Pujalte (2003), Sea-level, humidity, and land-erosion records across the initial Eocene thermal maximum from a continental-marine transect in northern Spain, *Geology*, *31*, 689–692.

Schmitz, B., and V. Pujalte (2007), Abrupt increase in season extreme precipitation at the Paleocene-Eocene boundary, *Geology*, *35*, 215–218.

Schouten, S., M. Woltering, W. I. C. Rijpstra, A. Sluijs, H. Brinkhuis, and J. S. Sinninghe Damsté (2007), The Paleocene–Eocene carbon isotope excursion in higher plant organic matter: Differential fractionation of angiosperms and conifers in the Arctic, *Earth Planet. Sci. Lett.*, *258*, 581–592.

Schumann, D., et al. (2008), Gigantism in unique biogenic magnetite at the Paleocene–Eocene Thermal Maximum, *Proc. Natl. Acad. Sci. USA*, *105*, 17,648–17,653.

Sluijs, A., et al. (2007), Environmental precursors to rapid light carbon injection at the Palaeocene/Eocene boundary, *Nature*, *450*, 1218–1221.

Snowball, I. F. (1994), Bacterial magnetite and the magnetic properties of sediments in a swedish lake, *Earth Planet. Sci. Lett.*, *126*, 129–142.

Storey, M., R. A. Duncan, and C. C. Swisher III (2007), Paleocene-Eocene Thermal Maximum and the opening of the Northeast Atlantic, *Science*, *316*, 587–589.

Svensen, H., S. Planke, A. Malthe-Sørenssen, B. Jamtveit, R. Myklebust, T. R. Eidem, and S. S. Rey (2004), Release of methane from a volcanic basin as a mechanism for initial Eocene global warming, *Nature*, *429*, 542–545.

Tarduno, J. A. (1994), Temporal trends of magnetic dissolution in the pelagic realm: Gauging paleoproductivity, *Earth Planet. Sci. Lett.*, *123*, 39–48.

Van Sickel, W. A., M. A. Kominz, K. G. Miller, and J. V. Browning (2004), Late Cretaceous and Cenozoic sea-level estimates: Backstripping analysis of borehole data, onshore New Jersey, *Basin Res.*, *16*, 451–465.

Wdowiak, T. J., L. P. Armendarez, D. G. Agresti, M. L. Wade, S. Y. Wdowiak, P. Claeys, and G. Izett (2001), Presence of an iron-rich nanophase material in the upper layer of the Cretaceous-Tertiary boundary clay, *Meteorit. Planet. Sci.*, *36*, 123–133.

Weiss, B. P., S. S. Kim, J. L. Kirschvink, R. E. Kopp, M. Sankaran, A. Kobayashi, and A. Komeili (2004), Ferromagnetic resonance and low temperature magnetic tests for biogenic magnetite, *Earth Planet. Sci. Lett.*, *224*, 73–89.

Zachos, J. C., S. Schouten, S. Bohaty, T. Quattlebaum, A. Sluijs, H. Brinkhuis, S. J. Gibbs, and T. J. Bralower (2006), Extreme warming of mid-latitude coastal ocean during the Paleocene-Eocene Thermal Maximum: Inferences from TEX86 and isotope data, *Geology*, *34*, 737–740.

Zachos, J. C., G. R. Dickens, and R. E. Zeebe (2008), An early Cenozoic perspective on greenhouse warming and carbon-cycle dynamics, *Nature*, *451*, 279–283.

R. E. Kopp, Department of Geosciences and Woodrow Wilson School of Public & International Affairs, Princeton University, Princeton, NJ 08544, USA. (rkopp@princeton.edu)

D. Schumann and H. Vali, Facility for Electron Microscopy Research, McGill University, 3640 University Street, Montreal, Quebec, H3A 2B2 Canada.

T. D. Raub, Division of Geological and Planetary Sciences, California Institute of Technology, Pasadena, CA 91125, USA.

D. S. Powars, U.S. Geological Survey, Reston, VA 20192, USA.

L. V. Godfrey, Institute of Marine and Coastal Sciences, Rutgers University, New Brunswick, NJ 08901, USA.

N. L. Swanson-Hysell and A. C. Maloof, Department of Geosciences, Princeton University, Princeton, NJ 08544, USA.
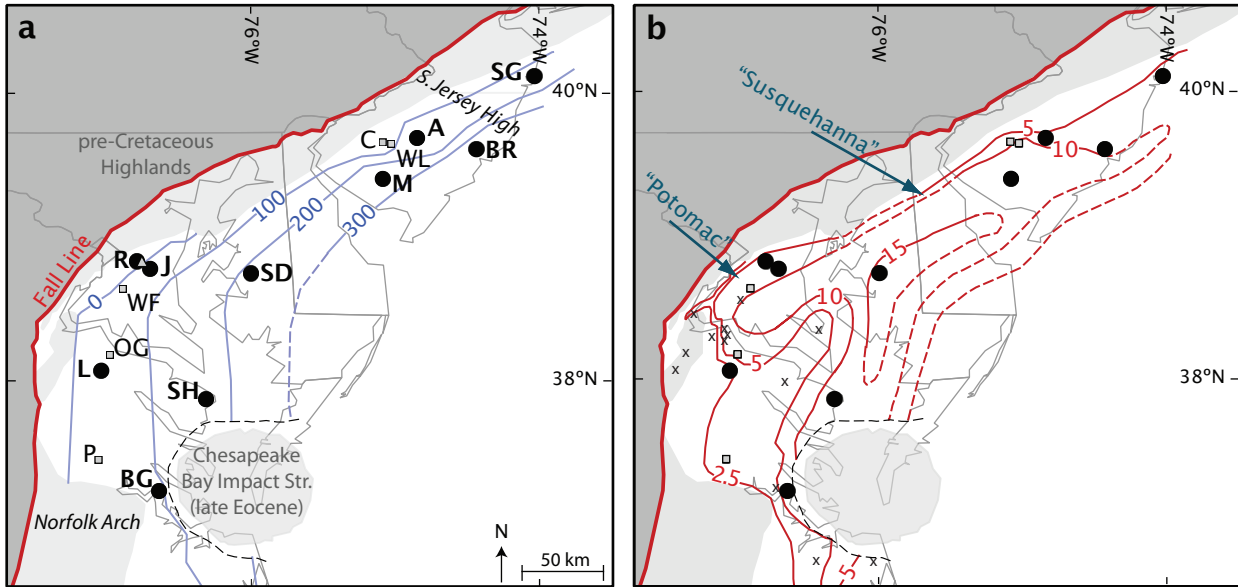
Figure 1. (a) Map of sites discussed in the text, superimposed upon the distribution (lightly shaded where not preserved) and basal structure contours (medium width lines, altitude in meters below sea level; dashed lines inferred in the absence of direct constraints) of the Marlboro Clay as compiled from *Powars and Bruce* [1999], initial reports for ODP legs 150X and 174AX, and unpublished data by Powars (2009). The heavy line marks the Fall Line. Circles represent core sites included in our analysis; squares represent other sites discussed. The triangle represents the location of the Upper Marlboro outcrop. (A—Ancora; BG—Busch Gardens; BR—Bass River; C–Clayton; J—Jackson Landing; L—Loretto; M—Millville; OG–Oak Grove; P–Putneys Mill; R—Randall's Farm; SD—South Dover Bridge; SG—Sea Girt; SH—Surprise Hill; WF–Waldorf; WL–Wilson Lake) (b) Isopachs (medium width lines, thickness in meters; dashed lines inferred in the absence of direct constraints) of the Marlboro Clay. Crosses mark cores that provide constraints but are not discussed in the text; constraints are also provided by auger cores (not shown). Approximate Paleogene positions of the paleo-Potomac and paleo-Susquehanna rivers based upon *Poag and Sevon* [1989] are indicated. Truncation or thinning of the Marlboro Clay on the uplifted side of faults and thickening in downdropped areas [*Mixon and Powars*, 1984] produce the irregularities in the isopachs in Virginia and Maryland. The dashed black line around the Chesapeake Bay Impact Structure represents the preserved limit of Paleogene sediments around the crater. While the impact has removed the Marlboro Clay across a large area of southeastern Virginia [*Powars and Bruce*, 1999], the clay is preserved to the south to about the Virginia–North Carolina state line.
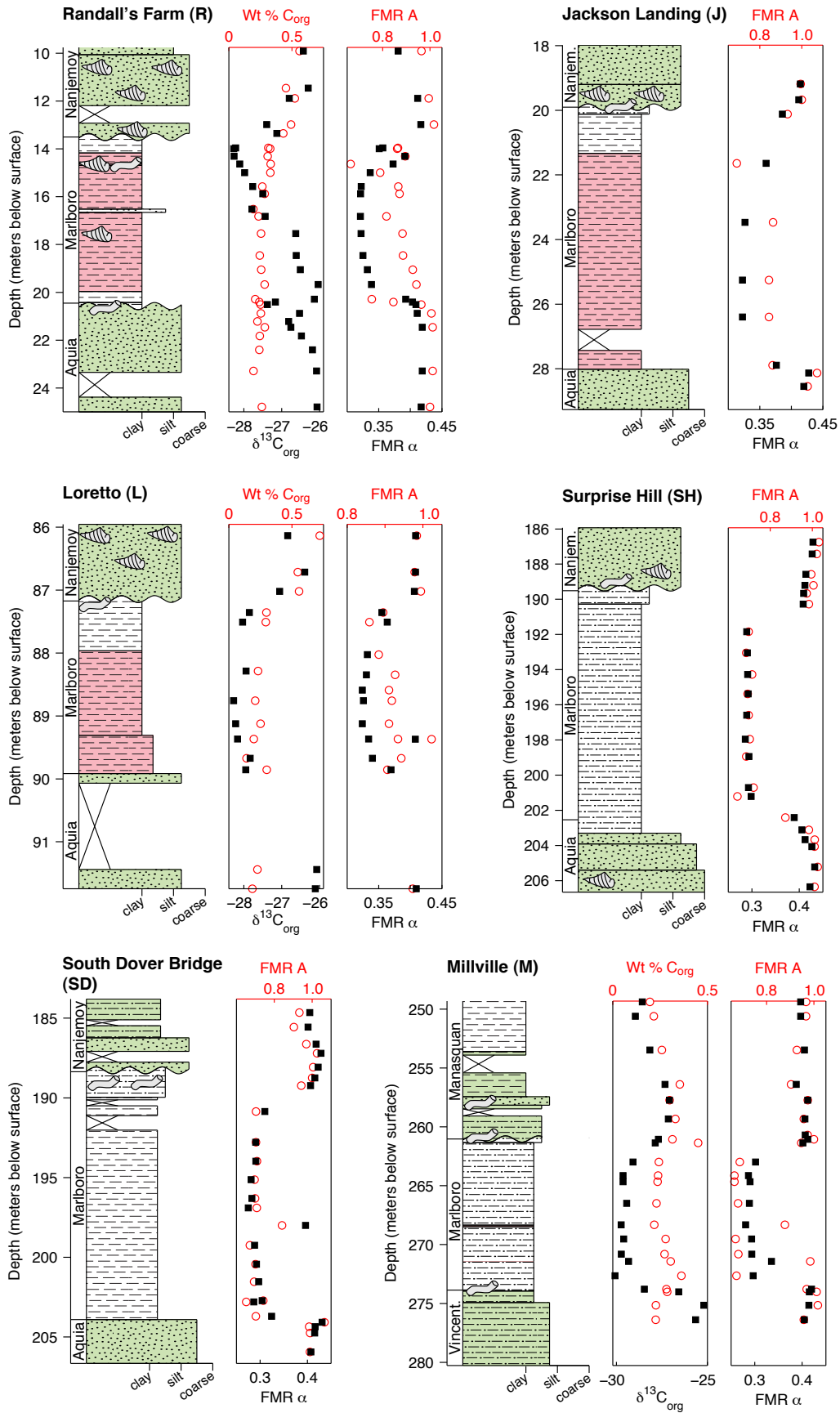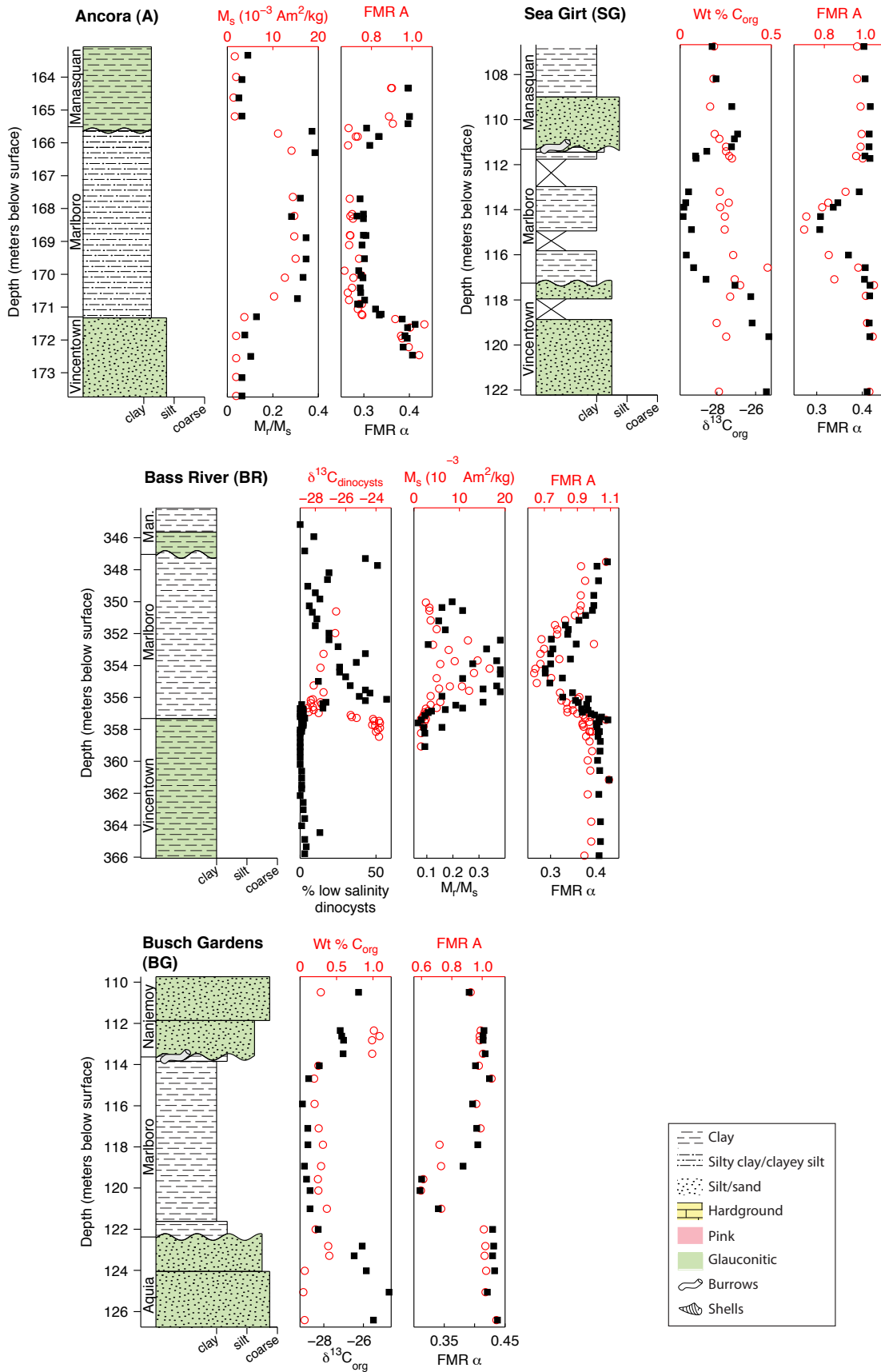
Figure 2. Stratigraphic logs, $\delta^{13}C_{org}$, C_{org} concentrations, and FMR parameters A and α for the Marlboro Clay and bounding sediments in the ten cores analyzed. Site codes are as in Figure 1. For BR, dinocyst organic carbon and low salinity dinocyst fraction data from *Sluijs et al.* [2007] are also shown. For A and BR, magnetic hysteresis data from *Kent et al.* [2003] are also shown.
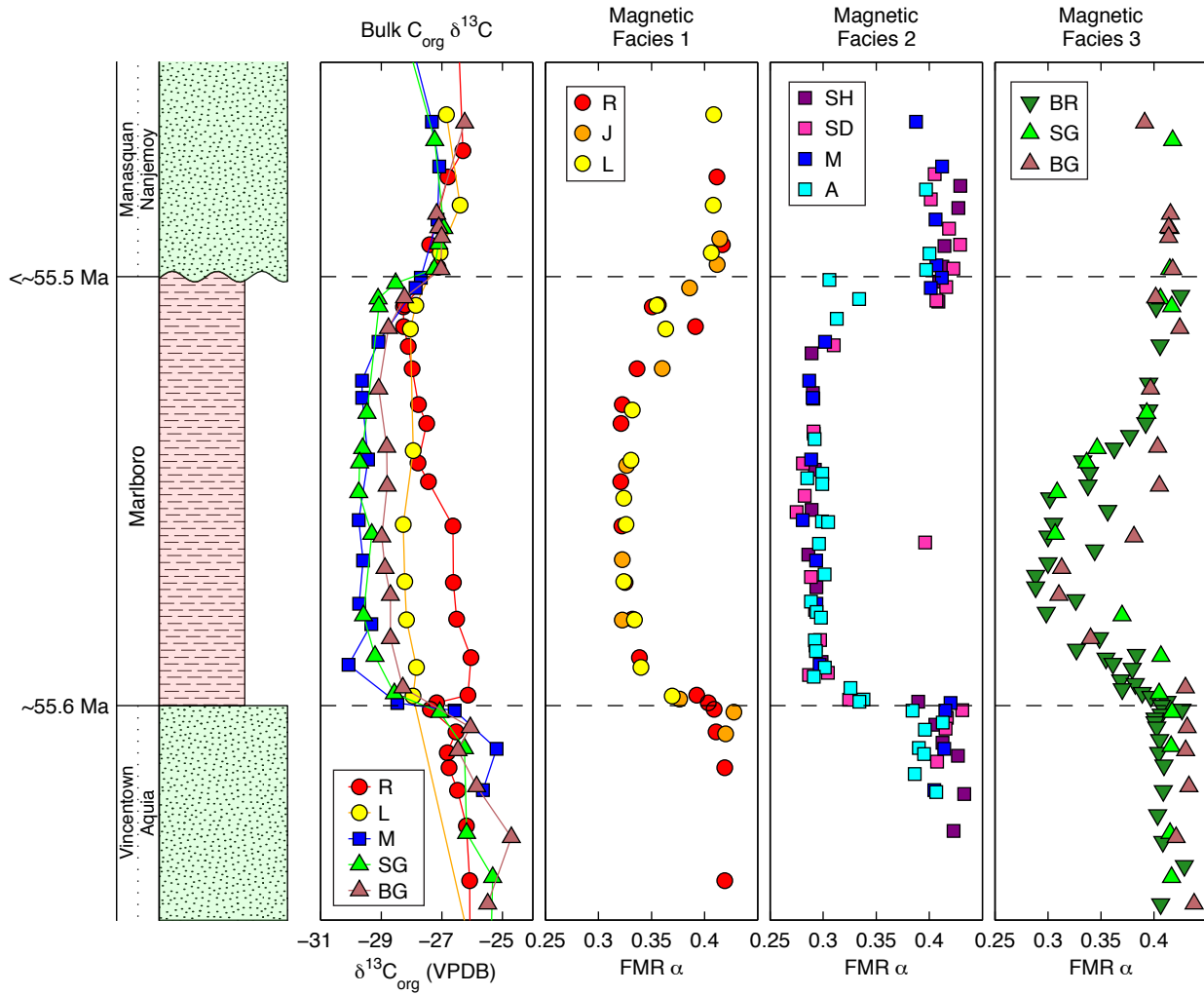
Figure 3. Profiles of α in each measured core, plotted alongside bulk organic carbon isotopes from several cores and a generalized stratigraphic column. Depths are normalized to the lithological thickness of the Marlboro.
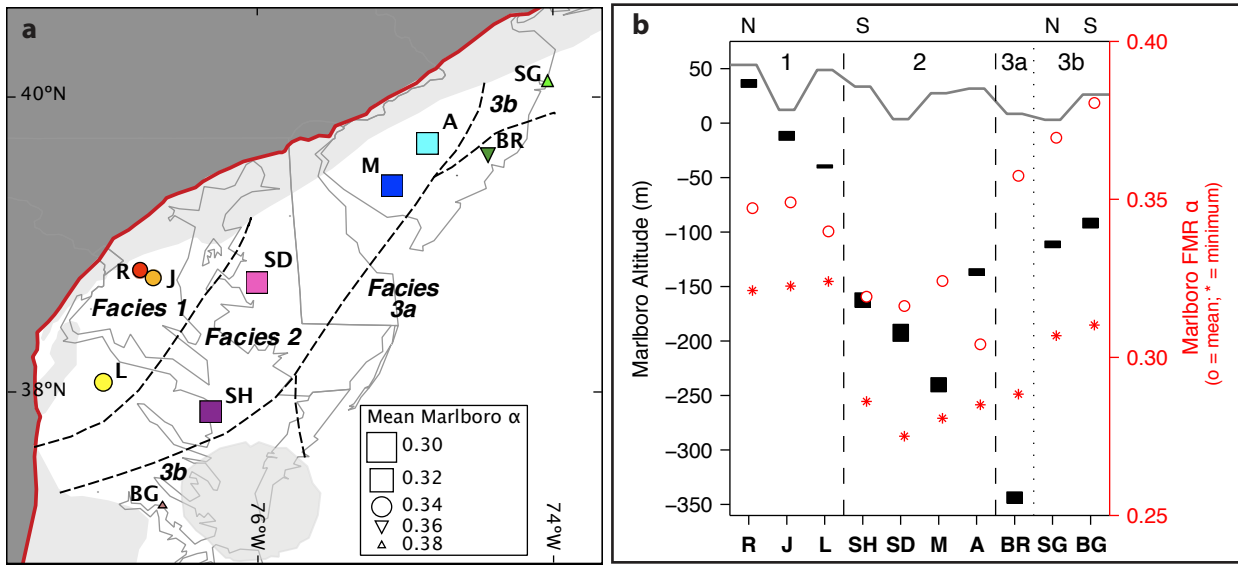
Figure 4. (a) Map of the minimum value of the FMR parameter α attained within the Marlboro Clay. The markers vary in size according to the mean value of α in the clay (see scale in legend) and in shape by facies, as in Figure 3. Dashed black lines demarcate the magnetic facies. (b) Positions and thicknesses of the Marlboro Clay at each site with respect to mean sea level (shown by the bars with relation to the left vertical axis). The thin gray profile marks the surface elevation. Circles mark mean α in the Marlboro Clay and stars mark the minimum α (shown with relation to the right vertical axis). Different facies are separated by vertical lines and identified at the top of the figure.
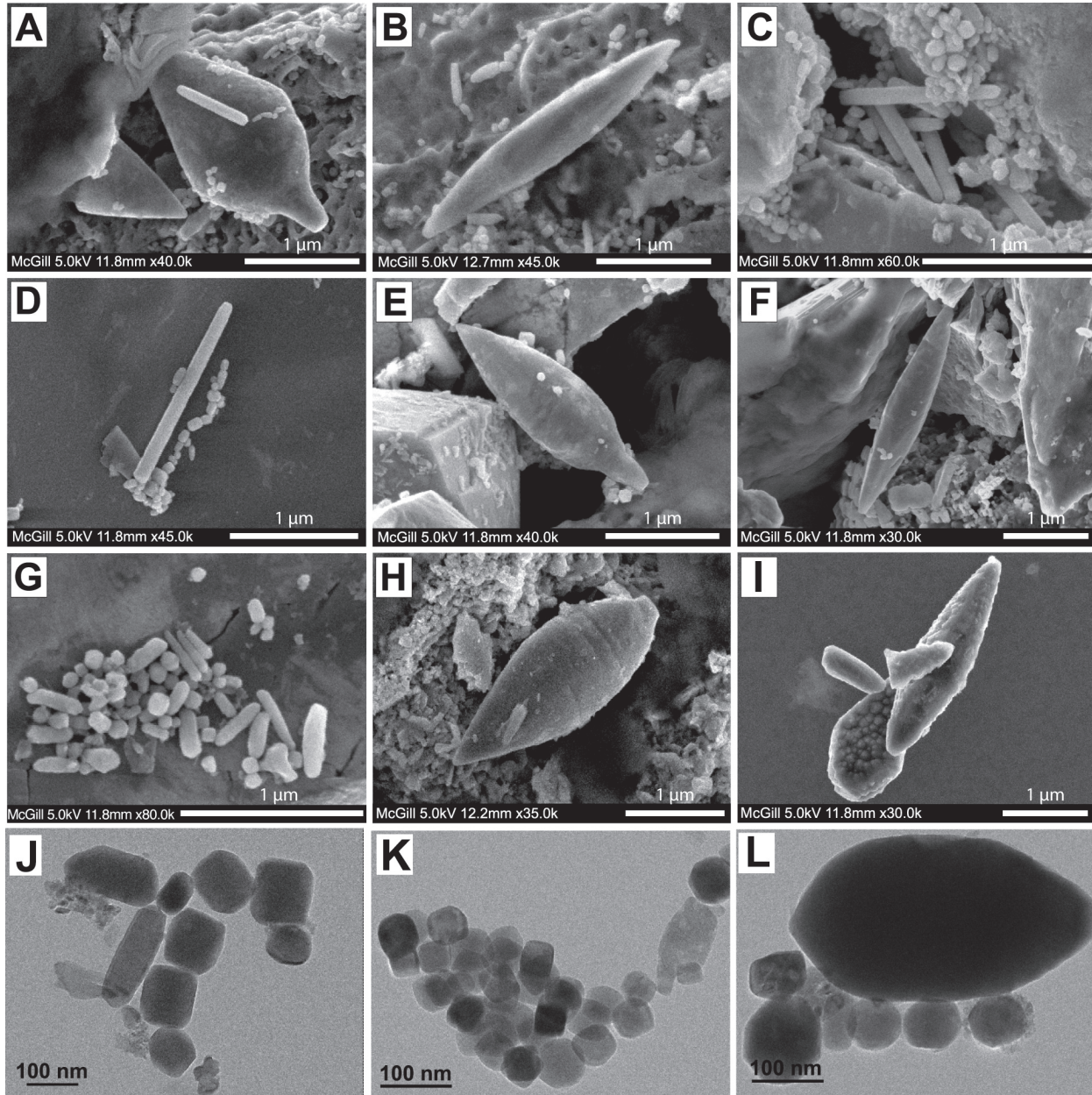
Figure 5. Electron micrographs of magnetic extracts from the Marlboro Clay. SEM images from Surprise Hill: (A) Spearhead magnetite particles, (B) spindle-shaped magnetite particle, (C) group of elongated hexaoctahedra surrounded by conventional bacterial magnetofossils, and (D) elongated hexaoctahedra and conventional bacterial magnetofossils in a chain-like arrangement. SEM images from Sea Girt: (E) Spearhead particle, (F) spindle-shaped particle, and (G) conventional bacterial magnetofossils. SEM image from Randall's Farm: (H) Spearhead particle. SEM image from Busch Gardens (sample BF-400.30, -95.8 m altitude): (I) spearhead and spindle-shaped magnetite particles with surface dissolution patterns. TEM images from Sea Girt: (J–K) conventional bacterial magnetofossils, and (L) conventional bacterial magnetofossils attached to a small spearhead crystal (large particle).
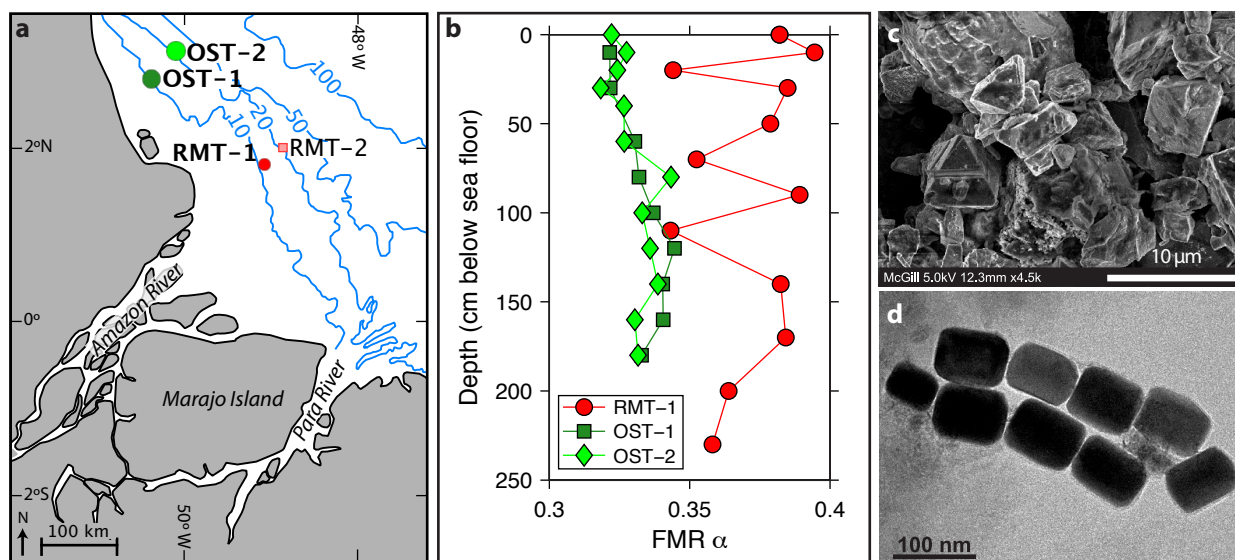
Figure 6. FMR and EM analysis of shallow neritic cores from the Amazon shelf. (a) Map of localities. Contour lines (from *Aller et al.* [1996]) show bathymetry in meters. (b) Profiles of the FMR parameter α. (c–d) SEM and TEM images of the magnetic extracts. A large proportion of the magnetic extracts are composed of detrital magnetic materials (c; from OST-1 at 35 cm). However, besides detrital magnetic grains these samples also contain (d) conventional bacterial magnetofossils with various known morphologies, as in the collapsed chain of elongated hexaoctahedra (from OST-2 at 35 cm). Additional SEM and TEM images are included in the Auxiliary Material.

An Appalachian Amazon? Magnetofossil evidence for the development
of a tropical river-like system in the mid-Atlantic U.S.
during the Paleocene-Eocene Thermal Maximum

Robert E. Kopp (1,2), Dirk Schumann (3), Timothy D. Raub (4),
David S. Powars (5), Linda V. Godfrey (6), Nicholas L. Swanson-Hysell (1),
Adam C. Maloof (1), and Hojatollah Vali (3,7)

(1) Department of Geosciences, Princeton University, Princeton, New Jersey, USA
(2) Woodrow Wilson School of Public and International Affairs, Princeton
University, Princeton, New Jersey, USA
(3) Department of Earth and Planetary Sciences and Facility for Electron
Microscopy Research, McGill University, Montréal, Québec, Canada
(4) Division of Geological and Planetary Sciences, California Institute of
Technology, Pasadena, California, USA
(5) United States Geological Survey, Reston, Virginia, USA
(6) Institute of Marine and Coastal Sciences, Rutgers University, New Brunswick,
New Jersey, USA
(7) Department of Anatomy & Cell Biology, McGill University, Montréal, Québec,
Canada

Introduction

This auxiliary material contains text dicussing the evaluation of the
idenitification of magnetofossils in the Marlboro Clay and an order-of-magnitude
discussion of the implications of the tropical river shelf analog for regional
precipitation. It also contains FMR data for the cores discussed in the main
text and stratigraphic, FMR, and rock magnetic data for the Upper Marlboro, MD,
outcrop (in Postscript format). It futher includes additional electron
micrographs of Marlboro Clay and Amazon Shelf samples (in JPEG format) beyond
those included in the main text and a table summarizing observations from
electron microscopy of the cores.

1. SText-Magnetofossils.tex Evaluation of the Marlboro Clay magnetofossil
identification against the criteria of Kopp and Kirschvink [2008].

2. SText-Precipitation.tex Order-of-magntitude calculation of the implications
of PETM discharge estimates regional precipitation.

3. SFig-FMRSpectra.eps FMR data for the cores analyzed in this study. The
position of the the units is as in Figure 2 of the main text. Altitude in meters
above sea level and depth in feet below surface are denoted on the y axes.
Within each core, total electron spin resonance absorption and relative
paramagnetic Fe(III) concentrations are shown in arbitrary units. Total
absorption is determined by integrating the derivative spectra across all
fields. Paramagnetic Fe(III) concentrations are derived from the height of the
g=4.3 (~160 mT) peak in the FMR spectra, as described in Maloof et al. [2007].
In these sediments, changes in paramagnetic Fe(III) content likely reflect clay
abundance. A subset of the raw FMR derivative spectra are also shown. For each
spectrum, the position of the baseline is placed at a vertical position
corresponding to depth in the core.

4. SFig-Outcrop.eps Stratigraphic and FMR data for the Upper Marlboro, MD, outcrop.

5. SFig-OutcropVsCore-IRM.eps Isothermal remanent magnetizations (IRM) for samples of the Marlboro Clay in the Upper Marlboro outcrop (red) and in the Randall's Farm (R, green) and Jackson Landing (J, blue) cores. IRM acquisition curves are shown at left and derived coercivity spectra are shown at right. IRM experiments were conducted on about 300-500 mg of crushed sediment powder in quartz glass tubes. Samples were imparted IRMs progressively in pulse fields up to 350 mT and measured using a 2G SQUID magnetometer as described in Kirschvink et al. [2008]. The IRM in outcrop material in an order of magnitude weaker than in core material, while the shift in peak coercivity indicates that the outcrop is dominated by high-coercivity ferric oxides such as goethite rather than the magnetite that characterizes core material.

5. SFig-DissolutionFeatures-TEM.jpg Transmission electron micrograph of an extensively altered spindle-shaped particle from sample BG-400.30 (122.0 m depth). The majority of spearheads and spindles from that sample show extensive alteration features on their surfaces, and TEM investigations revealed no conventional bacterial magnetofossils. The location of this sample (as well as sample SG-365.55 (111.7 m depth), which also lacks conventional magnetofossils) near the contacts of the Marlboro Clay suggests that burrowing or other processes associated with the contacts rendering these samples more susceptible to reductive dissolution.

6. SFig-Amazon-EM-additional.jpg Additional SEM and TEM images of the magnetic extracts from the shallow neritic core samples from the Amazon Shelf. (A) Detrital magnetic material from RMT-1 at 35 cm. (B) Dispersed particles with a hexagonal base and (C) bullet-shaped particles from OST-2 at 145 cm.

7. STable-Marlboro-EM-Observations.xls and STable-Marlboro-EM-Observations.txt Qualitative and semi-quantitative electron microscopy observations of the abundance of magnetic particles in magnetic extracts. Where present, numerical counts of putative eukaryotic magnetofossils are based upon the number of particles in a magnetic extract observed under SEM on a single Cu grid within a ~40 micron by 50 micron frame. Observations of conventional magnetofossils are based on TEM. + indicates presence; ++ indicates high abundance; - indicates absence; blanks and ? indicate missing or inconclusive observations.

    7.1 Column "core", core from which sample comes. (R--Randall's Farm. SH--Surprise Hill. A--Ancora. SG--Sea Girt. BG--Busch Gardens)
    7.2 Column "depth", feet below surface, depth of sample in core.
    7.3 Column "altitude", meters below mean sea level, altitude of sample.
    7.4 Column "unit", stratigraphic unit.
    7.5 Column "alpha", FMR alpha value of sample.
    7.6 Column "spearhead", abundance of spearhead magnetite particles.
    7.7 Column "spindle", abundance of spindle-shaped magnetite particles.
    7.8 Column "elongated_hexaoctahedra", abundance of large elongated hexaoctahedral magnetite particles.
    7.9 Column "conventional", abundance of conventional bacterial magnetofossils.
    7.10 Column "detrital", abundance of detrital magnetic particles.

REFERENCES

J. L. Kirschvink, R. E. Kopp, T. D. Raub, C. T. Baumgartner, and J. W. Holt

(2008). Rapid, precise, and high-sensitivity acquisition of paleomagnetic and rock-magnetic data: Development of a low-noise automatic sample changing system for superconducting rock magnetometers. Geochem. Geophys. Geosys. 9: Q05Y01, doi:10.1029/2007GC001856.

R. E. Kopp and J. L. Kirschvink (2008). The identification and biogeochemical interpretation of fossil magnetotactic bactery. Earth Sci. Rev. 86: 42-61, doi: 10.1016/j.earscirev.2007.08.001

A. C. Maloof, R. E. Kopp, J. P. Grotzinger, D. A. Fike, T. Bosak, H. Vali, P. M. Poussart, B. P. Weiss, and J. L. Kirschvink (2007). Sedimentary iron cycling and the origin and preservation of magnetization in platform carbonate muds, Andros Island, Bahamas. Earth Planet. Sci. Lett. 259: 581-598, doi:10.1016/j.epsl. 2007.05.021

A. Sluijs, et al. Subtropical Arctic Ocean termperatures during the Paleocene/ Eocene thermal maximum. Nature 450: 1218-1221, doi:10.1038/nature06400.

Evaluating magnetofossil identifications

Kopp and Kirschvink (2008) presented a scheme for evaluating putative magnetofossil identifications based upon six axes: sedimentary context, the presence of a single doman magnetic phase, particle size and shape, the robustness of evidence for chains, the chemical purity of particles, and the crystallographic perfection of particles. The first axis, context, is used to establish how strong other lines of evidence need to be in order to declare an identification robust. This threshold is raised if sediments have undergone burial metamorphism or reflect a setting with no younger magnetofossil-bearing analogs. In the case of the Marlboro Clay, the sediments are unmetamorphosed and analogous to younger sediments known to contain magnetofossils (other marine clays).

The second axis is magnetic or microscopic evidence for a single domain magnetic phase. Without such evidence, a putative magnetofossil identification is considered a failure. This criterion was satisfied by the magnetic and TEM work of *Lanci et al.* (2002) and *Kent et al.* (2003).

The third axis, size and shape, is weighted more heavily than the subsequent three. Four criteria contribute to this axis: (1) coercivity or FMR spectra indicating narrow size and shape distribution, (2) TEM evidence for single domain particles with the truncated crystal edges characteristic of the crystals produced by many magnetotactic bacteria, (3) TEM evidence for elongate single domain particles, which are produced by many magnetotactic bacteria, and (4) statistical TEM evidence for populations of crystals with narrow size and shape distributions. *Kopp et al.* (2007) and *Lippert and Zachos* (2007) established that the Marlboro Clay magnetofossil met all four of these criteria.

The fourth axis, chains, grades the quality of chain identification on a scale from zero to four. The most basic evidence for chains (score of 1) can come from either suggestive SEM or low-temperature thermal demagnetization results. A score of two reflects either evidence for chains from FMR spectra (*Kopp et al.*, 2006) or from short chains of particles from a single size and shape distribution observed in TEM of magnetic extracts. Because short chain-like arrangements might form during sample preparation, these TEM observations by themselves are not regarded as conclusive. A score of three reflects the combination of TEM images of short chains and FMR data indicating that chains are a major in-situ component. It can also reflect the TEM observation of long chains from a single size and shape distribution. The highest score, four, is awarded only to samples that combine TEM images of long chains with evidence from either FMR or SEM for their in situ occurrence. On this axis, the Marlboro Clay receives a three for its combination of TEM images of short chains and FMR evidence of their in situ occurrence.

The fifth axis, chemical purity, and sixth axis, crystallographic perfection, each award one point. Assessments of chemical purity can be based on microanalytic techniques such as energy dispersive X-ray spectroscopy (EDS), as presented for the Marlboro Clay by *Schumann et al.* (2008). Crystallographic perfection can be established by high-resolution TEM, as done by *Kopp et al.* (2007).

Kopp and Kirschvink (2007) presented an algorithm for projecting the last four axes onto a single scale ranging from zero to eighteen. This algorithm adds three times the value of the third (size and shape) axis to the sum of the fourth through sixth axes (chains, chemical purity, and crystallographic perfection). The thresholds for the robustness of identifications vary based upon sedimentary context. For settings analogous to younger magnetofossil-bearing settings, the threshold is 9 with robust primary paleomagnetic data, 10 in the absence of such data (as in the Marlboro Clay), and 13 for settings that are remagnetized or metamorphosed. Environments without younger analogs, such as a Martian basalt, have a threshold score of 17.

On this scale, the Marlboro Clay bacterial magnetofossils receive a score of 17/18, the second highest received by any magnetofossils reported in the literature (*Kopp and Kirschvink*, 2008).

References

Kent, D. V., B. S. Cramer, L. Lanci, D. Wang, J. D. Wright, and R. Van der Voo (2003), A case for a comet impact trigger for the Paleocene/Eocene thermal maximum and carbon isotope excursion, *Earth and Planetary Science Letters*, *211*, 13–26.

Kopp, R. E., and J. L. Kirschvink (2007), A scoring scheme for evaluating magnetofossil identifications, *Eos Trans. AGU*, *88*, Fall Meet. Suppl., Abstract GP43B–1218.

Kopp, R. E., and J. L. Kirschvink (2008), The identification and biogeochemical interpretation of fossil magnetotactic bacteria, *Earth-Science Reviews*, *86*, 42–61.

Kopp, R. E., B. P. Weiss, A. C. Maloof, H. Vali, C. Z. Nash, and J. L. Kirschvink (2006), Chains, clumps, and strings: Magnetofossil taphonomy with ferromagnetic resonance spectroscopy, *Earth and Planetary Science Letters*, *247*, 10–25.

Kopp, R. E., T. D. Raub, D. Schumann, H. Vali, A. V. Smirnov, and J. L. Kirschvink (2007), Magnetofossil spike during the Paleocene-Eocene thermal maximum: Ferromagnetic resonance, rock magnetic, and electron microscopy evidence from Ancora, New Jersey, United States, *Paleoceanography*, *22*, PA4103, doi:10.1029/2007PA001473.

Lanci, L., D. V. Kent, and K. G. Miller (2002), Detection of Late Cretaceous and Cenozoic sequence boundaries on the Atlantic coastal plain using core log integration of magnetic susceptibility and natural gamma ray measurements at Ancora, New Jersey, *Journal Of Geophysical Research*, *107*, 2216.

Lippert, P. C., and J. C. Zachos (2007), A biogenic origin for anomalous fine-grained magnetic material at the Paleocene-Eocene boundary at Wilson Lake, New Jersey, *Paleoceanography*, *22*, PA4104, doi:10.1029/2007PA001471.

Schumann, D., et al. (2008), Gigantism in unique biogenic magnetite at the Paleocene–Eocene Thermal Maximum, *Proceedings of the National Academy of Sciences*, *105*, 17,648–17,653, doi:10.1073/pnas.0803634105.

Implications of PETM Discharge Estimate for Regional Precipitation

Riverine discharge scales approximately linearly with integrated precipitation over a watershed area (*Galster*, 2007; *Saenger et al.*, 2006), though watershed geology, vegetation, and non-vegetative evaporative balance also play a role. Our estimate that the paleo-Potomac and paleo-Susquehanna rivers discharged roughly one-quarter of the sediment input of the modern Amazon during the PETM therefore implies a significant increase in regional precipitation relative to the latest Paleocene. An order-of-magnitude estimate for this increase can be crudely approximated as follows.

The modern Amazon River discharges $\sim$ 1200 million tons/y of suspended sediment (*Meade et al.*, 1985). One quarter of this value is $\sim$ 300 million tons/y. By comparison, the combined non-hurricane suspended sediment discharge of the Susquehanna River and the Potomac River today is about 2 million tons/y (*Gross et al.*, 1978; *U.S. Geological Survey*, 1996). The Susquehanna and Potomac watersheds currently have a combined area of about 112,000 km^2. If we include in the watershed all rivers currently draining into the Salisbury Embayment, as well as the Finger Lakes and Champlain lowland, which probably drained into the embayment before the Pleistocene, we expand this area to about 288,000 km^2 (*Pazzaglia and Brandon*, 1996). Non-hurricane suspended sediment discharge from this enlarged watershed under modern conditions would be expected to be about 5 million tons/y. To scale precipitation sufficiently to increase this value to 300 million tons/y would require an implausible level of precipitation (about 60 m/y).

Such an interpretation, however, assumes that the same linear relationship applies between precipitation and discharge during the PETM as applies when excluding hurricanes in the modern. Yet sediment discharge from flood events associated with hurricanes and tropical storms currently dominates discharge in the mid-Atlantic United States. Between 1966 and 1976, two hurricane-associated floods accounted for about a total of about 40 million tons of discharge from the Susquehanna River, an average of 20 million tons per flood (*Gross et al.*, 1978). Scaled to the enlarged watershed, this amounts to about 80 million tons per flood. It would take four such events a year to exceed 300 million tons of discharge. Less severe but more protracted flood events could also be responsible.
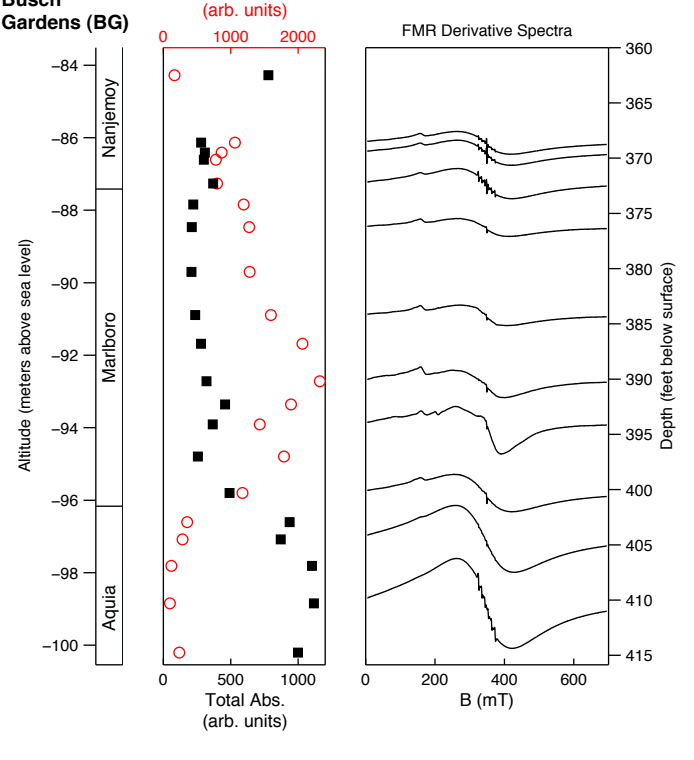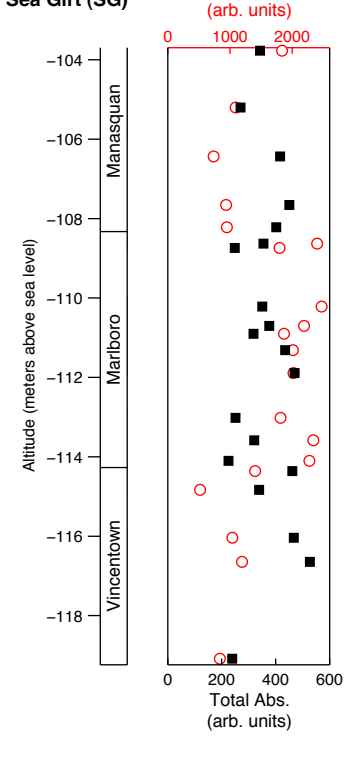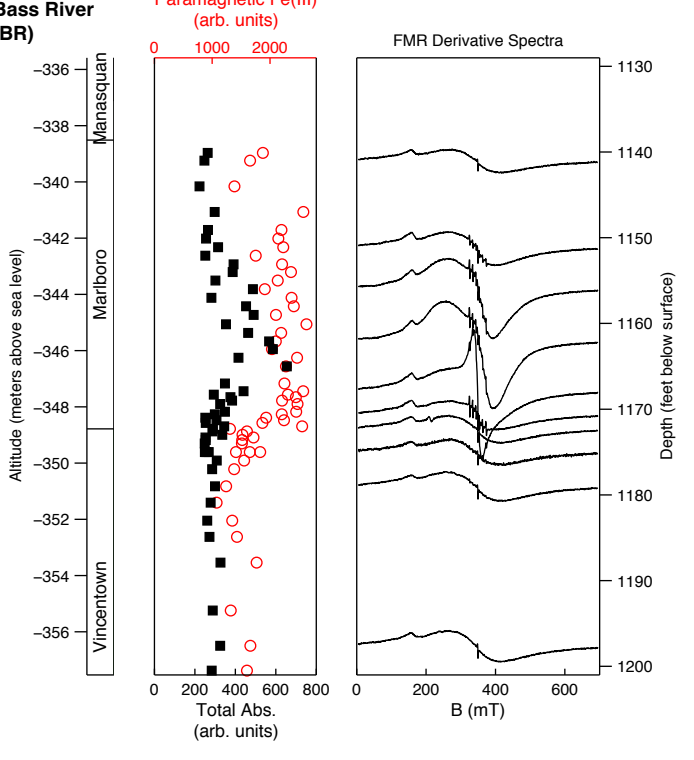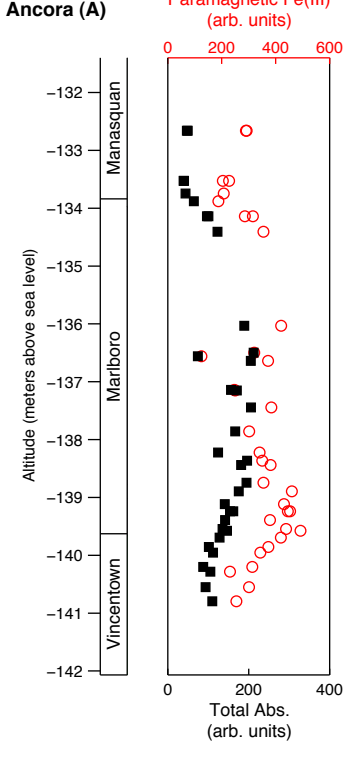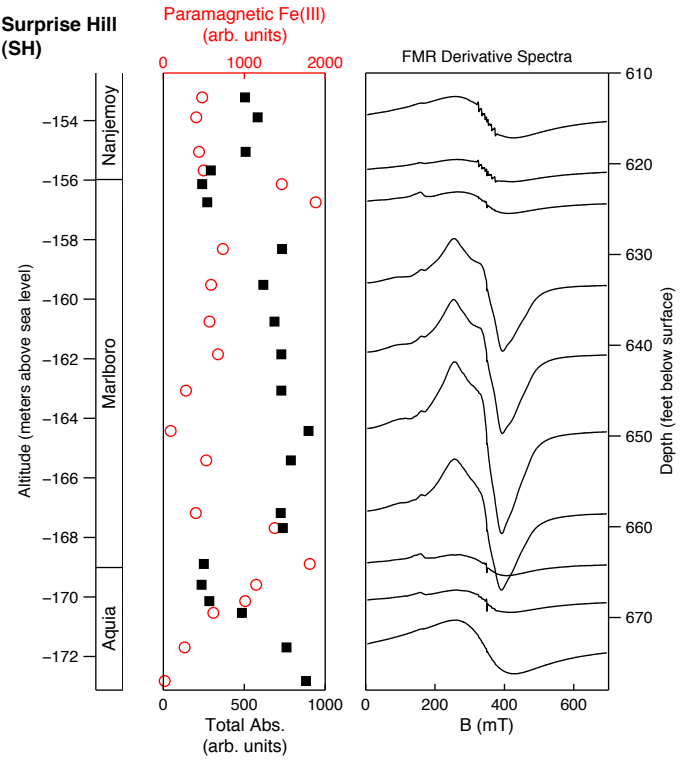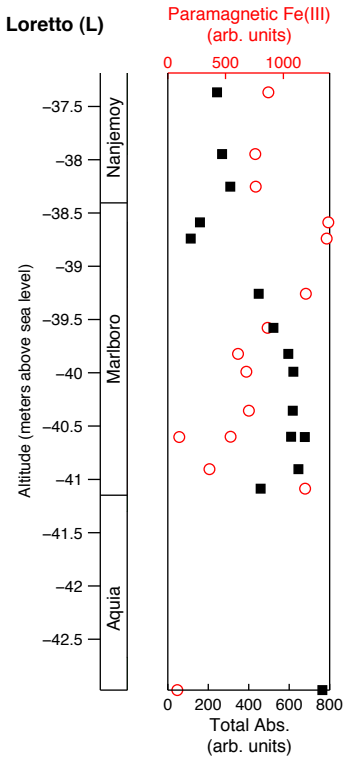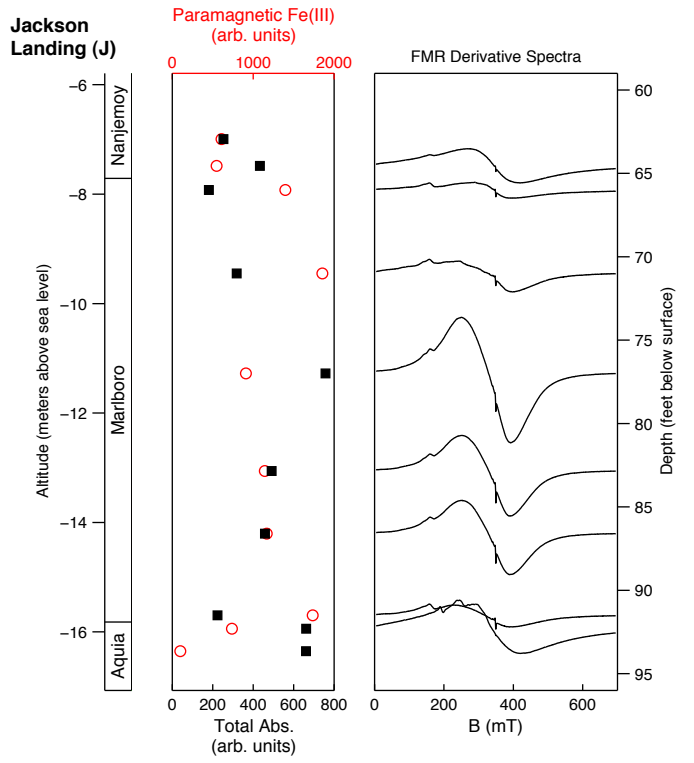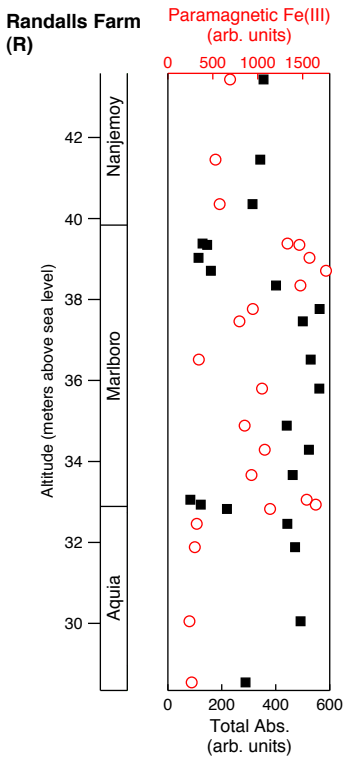
These inferences are consistent with prior suggestions of monsoonal precipitation patterns in New Jersey (*Zachos et al.*, 2006). However, that suggestion was based on the sparsity of terrestrial organic carbon in the Marlboro Clay at Wilson Lake, a finding that needs to be reconciled with sporomorphs and other plant material occasionally present in the Marlboro Clay in Maryland and Virginia.

More frequent tropical cyclones have been proposed as a mechanism for reducing the pole-to-equator temperature gradient during periods of globally warm climates (e.g., *Korty et al.*, 2008). If they occurred, they would be expected to leave a signal in the coastal environments of the northwest Atlantic

Ocean. The development of a tropical river shelf-like environment in the Salisbury Embayment may be such a signal.

References

Galster, J. (2007), Natural and anthropogenic influences on the scaling of discharge with drainage area for multiple watersheds, *Geosphere*, *3*, 260–271.

Gross, M., M. Karweit, W. Cronin, and J. Schubel (1978), Suspended sediment discharge of the Susquehanna River to northern Chesapeake Bay, 1966 to 1976, *Estuaries*, *1*, 106–110.

Korty, R., K. Emanuel, and J. Scott (2008), Tropical cyclone–induced upper-ocean mixing and climate: Application to equable climates, *Journal of Climate*, *21*, 638–654.

Meade, R., T. Dunne, J. Richey, U. de M. Santos, and E. Salati (1985), Storage and remobilization of suspended sediment in the lower Amazon River of Brazil, *Science*, *228*, 488–490.

Pazzaglia, F., and M. Brandon (1996), Macrogeomorphic evolution of the post-Triassic Appalachian mountains determined by deconvolution of the offshore basin sedimentary record, *Basin Research*, *8*, 255–278.

Saenger, C., T. Cronin, R. Thunell, and C. Vann (2006), Modelling river discharge and precipitation from estuarine salinity in the northern Chesapeake Bay: application to Holocene palaeoclimate, *The Holocene*, *16*, 467–477.

U.S. Geological Survey (1996), Suspended-sediment database, http://co.water.usgs.gov/sediment/.

Zachos, J. C., S. Schouten, S. Bohaty, T. Quattlebaum, A. Sluijs, H. Brinkhuis, S. J. Gibbs, and T. J. Bralower (2006), Extreme warming of mid-latitude coastal ocean during the paleocene-eocene thermal maximum: Inferences from tex86 and isotope data, *Geology*, *34*, 737–740.
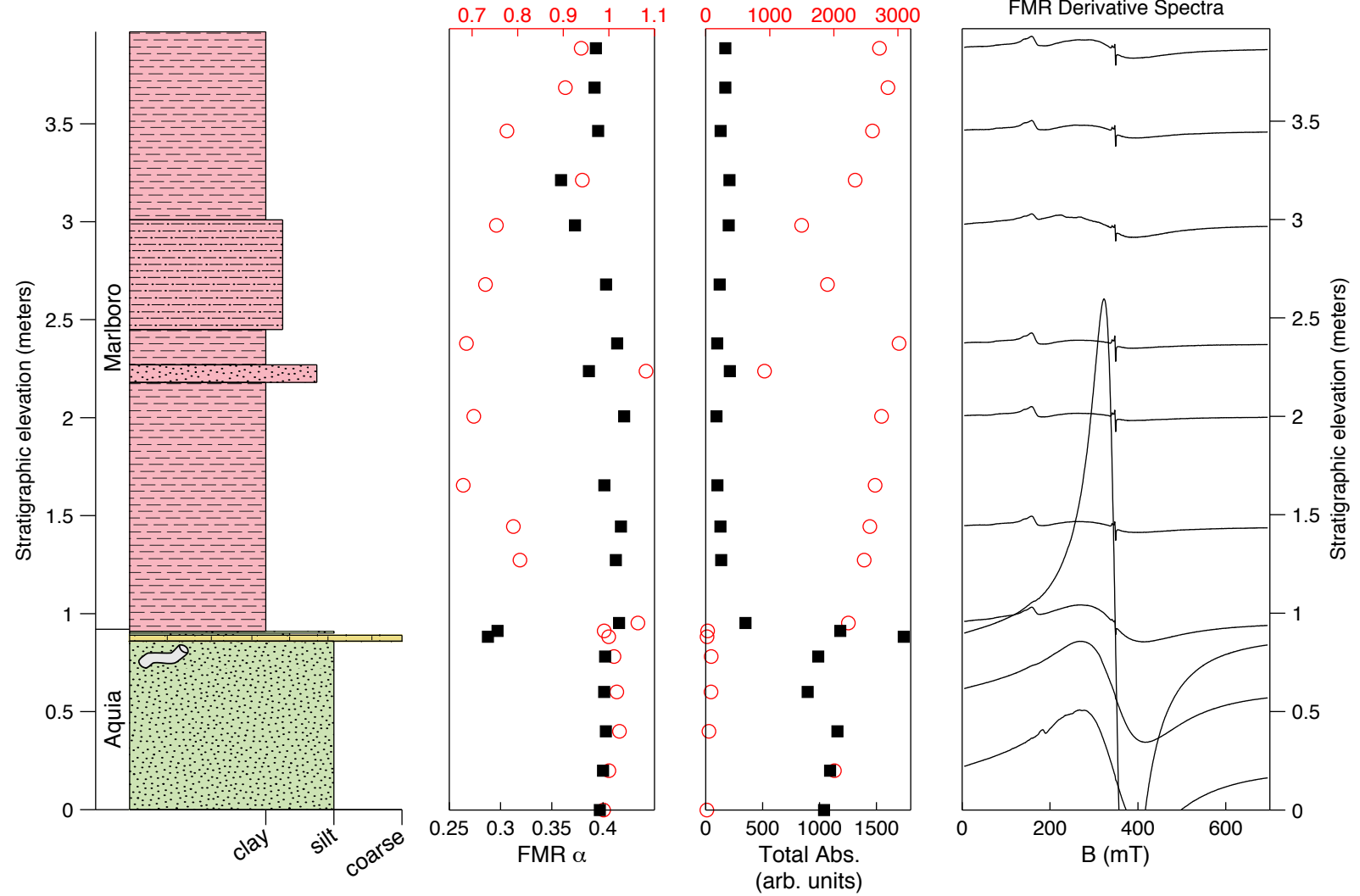
Randalls Farm (R)

Jackson Landing (J)

Loretto (L)

Surprise Hill (SH)

South Dover Bridge (SD)

Millville (M)

Ancora (A)

Bass River (BR)

Sea Girt (SG)

Busch Gardens (BG)

Upper Marlboro Outcrop

Marlboro

Aquia

Stratigraphic elevation (meters)

clay   silt   coarse

FMR A

0.7 0.8 0.9 1 1.1
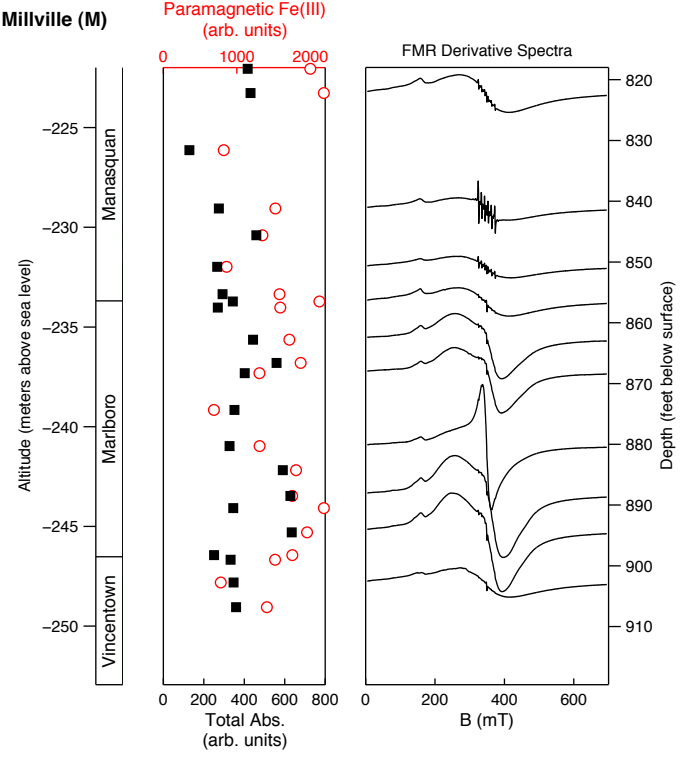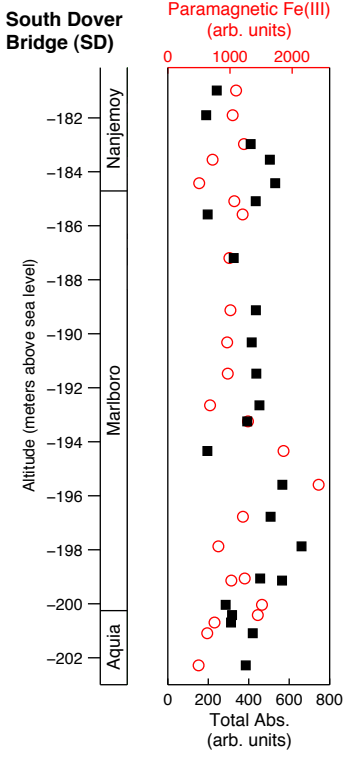
Paramagnetic Fe(III)
(arb. units)

0   1000   2000   3000

FMR Derivative Spectra

0.25   0.3   0.35   0.4

FMR α

0   500   1000   1500

Total Abs.
(arb. units)

0   200   400   600

B (mT)

Stratigraphic elevation (meters)

500 nm

A McGill 5.0kV 12.2mm x13.0k   4 micrometer

B 100 nm
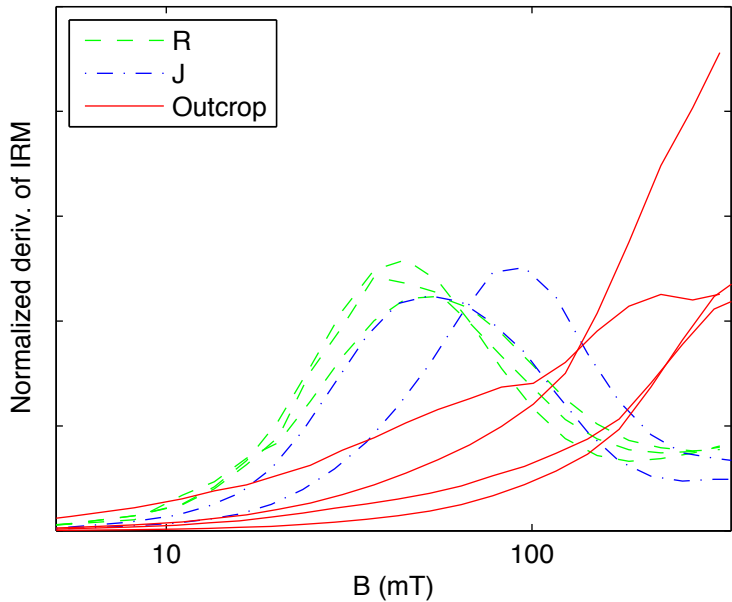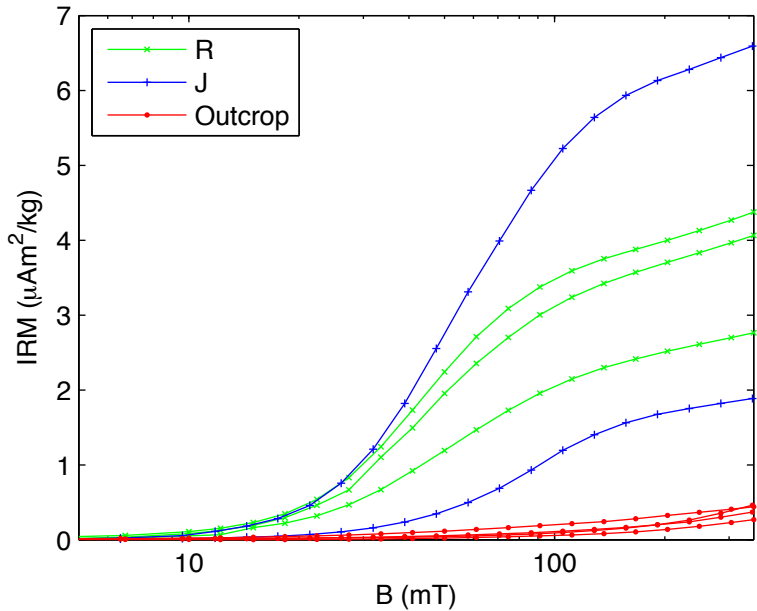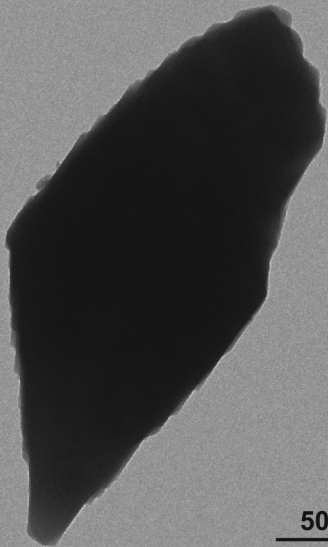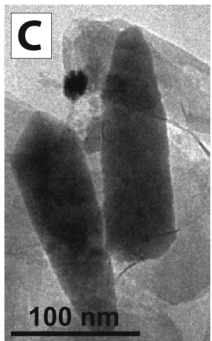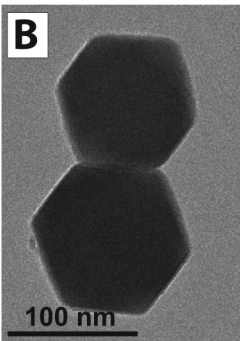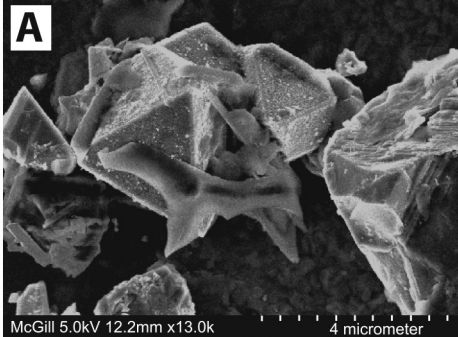
C 100 nm

Qualitative and semi-quantitative electron microscopy observations of the abundance of magnetic particles in magnetic extracts.

Core	Depth (feet)	Altitude (meters)	unit	α	spearhead	spindle	elongated hexaoctahedra	conventional	detrital material
R	42.60	40.36	Nanjemoy	0.42	-	-	-	-	-
R	43.80	39.99	Nanjemoy		-	-	-	-	-
R	45.80	39.38	Marlboro	0.36	?	?	+	+	+
R	57.55	35.80	Marlboro	0.32	+	?	?	+	++
R	63.50	33.99	Marlboro		+	?	+	+	++
R	66.55	33.06	Marlboro	0.39	-	-	-	-	+
R	68.50	32.46	Aquia	0.41	-	-	-	-	-
SH	622.25	-156.13	Marlboro	0.41	-	-	-	-	-
SH	641.00	-161.85	Marlboro	0.29	++	++	++	++	++
SH	660.15	-167.69	Marlboro	0.30	290	22	97	++	++
SH	666.40	-169.59	Aquia	0.41	-	-	-	?	-
A	541.98	-133.53	Manasquan	0.40	-	-	-	+	
A	543.14	-133.88	Manasquan	0.31	-	-	-	+	
A	543.99	-134.14	Marlboro	0.33	-	-	-	+	
A	550.20	-136.03	Marlboro	0.29	++	++	++	++	
A	551.73	-136.50	Marlboro	0.30	++	++	++	++	
A	553.84	-137.14	Marlboro	0.30	++	++	++	++	
A	553.87	-137.15	Marlboro	0.30	++	++	++	++	
A	554.83	-137.44	Marlboro	0.30	++	++	++	++	
A	556.19	-137.86	Marlboro	0.30	++	++	++	++	
A	557.39	-138.22	Marlboro	0.29	++	++	++	++	
A	557.85	-138.36	Marlboro	0.29	++	++	++	++	
A	559.10	-138.74	Marlboro	0.29	++	++	++	++	
A	559.59	-138.89	Marlboro	0.29	++	++	++	++	
A	560.72	-139.24	Marlboro	0.29	++	++	++	++	
A	561.73	-139.55	Marlboro	0.34	-	-	-	++	
A	564.15	-140.28	Manasquan	0.40	-	-	-	+	
A	568.10	-141.49	Manasquan		-	-	-	+	
SG	364.85	-108.22	Manasquan	0.42	-	-	-	?	
SG	366.55	-108.74	Marlboro	0.42	111	14	41	-	+
SG	373.65	-110.90	Marlboro	0.34	151	22	56	++	+
SG	376.90	-111.89	Marlboro	0.31	127	15	19	++	++
SG	382.45	-113.58	Marlboro	0.41	-	-	-	-	+
BG	380.30	-89.70	Marlboro	0.40	-	-	-	-	-
BG	390.20	-92.72	Marlboro	0.38	237	105	440	++	++
BG	394.10	-93.91	Marlboro	0.31	208	77	205	++	++
BG	400.30	-95.80	Marlboro	0.43	112	19	14	-	+
BG	402.95	-96.61	Aquia	0.43	-	-	-	?	-

Where present, counts are based on the number of particles in a magnetic extract on a single grid observed under SEM.
+ indicates presence; ++ indicates high abundance; - indicates absence; blanks and ? indicate missing or inconclusive observations.
Observations of conventional magnetofossils are based on TEM. Other observations are based on SEM.
(R--Randall's Farm. SH--Surprise Hill. A--Ancora. SG--Sea Girt. BG--Busch Gardens)